Received <day> <Month>, <year>; | Revised <day> <Month>, <year>; | Accepted <day> <Month>, <year>

DOI: xxx/xxxx

ARTICLE TYPE

A non-invasive system-level model order reduction scheme for flexible multibody simulation

Frank Naets*[1,2] | Thijs Devos[1,2] | Alexander Humer[3] | Johannes Gerstmayr[4]

[1]Member of DMMS Lab, Flanders Make @ KU Leuven
[2]Department of Mechanical Engineering, KU Leuven, Celestijnenlaan 300, 3001 Heverlee, Belgium
[3]Institute of Technical Mechanics, Johannes Kepler University,Altenberger Straße 69, 4040 Linz, Austria
[4]Institute of Mechatronics, University of Innsbruck, Technikerstraße 13, 6020 Innsbruck, Austria

Correspondence
*Frank Naets, Celestijnenlaan 300, 3001 Heverlee, Belgium. Email: frank.naets@kuleuven.be

Abstract

This paper presents a novel system-level model order reduction scheme for flexible multibody simulation, namely the System Level Affine Projection (SLAP). Contrary to existing system level model order reduction approaches for multibody systems simulation, this methodology allows to obtain a constant reduced order basis which can be obtained in a non-invasive fashion with respect to the original flexible multibody model. It is shown that this scheme enables an automatic joint constraint elimination which can be obtained at low computational cost through exploitation of the component level modes typically employed in flexible multibody simulation. The equations of motion are derived such that the computational cost of the resulting SLAP model is independent of the original model size. This approach results in a set of ordinary differential equations with a constant mass matrix and nonlinear internal forces. This structure makes the resulting model suitable for a range of estimation, control, and design applications. The proposed approach is validated numerically on a flexible four-bar mechanism and shows good accuracy for a very low order SLAP model.

KEYWORDS:
flexible multibody; model reduction; nonlinear

1 | INTRODUCTION

Over the past decades flexible multibody simulation has demonstrated itself as a powerful framework for the dynamic analysis of mechanical systems consisting of multiple components. For many industrial applications, the small deformation assumption in particular has led to the development of range of efficient descriptions like the floating-frame-of-reference component mode synthesis (FFR-CMS)[1,2] and generalized component mode synthesis approaches (GCMS)[3,4], and more recently the flexible natural coordinate formulation (FNCF)[5]. The possibility of these methods for effectively describing the system level dynamics at a feasible computational cost, in contrast to more general nonlinear finite element approaches, has led to an increasing interest in exploiting (flexible) multibody simulation paradigms in a range of novel frameworks like:

- Model based state-estimation[6,7,8];
- Model based control and design[9].

However, the broad application of these general frameworks for multibody system models faces two main difficulties:

- Many of the exploited methodologies developed for estimation and control, assume an ordinary differential equation (ODE) description for the underlying model.
- As many of these technologies are aimed toward fast/online or multi-query settings, model size and simulation cost is are ever important issues.

Current flexible multibody approaches however, typically lead to differential algebraic equations (DAE) with tens to hundreds of degrees-of-freedom, even after component level model order reduction. This differential algebraic structure can be resolved into a set of ordinary differential algebraic equations through a penalty formulation[8], instead of a Lagrange multiplier formulation, but this is often a numerically poorly conditioned approach and has several issues when redundant rotational parameterizations (like the ominous Euler parameters) are employed.

Model order reduction on a component level has been broadly investigated[10,11] and is a standard in flexible multibody simulation, e.g. through the *modal neutral file* interface with finite element software[12]. However, the number of degrees-of-freedom for a full system model is typically still high due to the numerous components and the requirement to properly resolve the interface conditions between the different components through dedicated interface modes.

In order to alleviate the issues above, this work proposes a system level reduced order flexible multibody formulation. This method is denoted as System Level Affine Projection (SLAP) as it relies on an affine projection from the reduced order DOFs to the system level global multibody coordinates. This approach allows to describe general fixed topology flexible multibody problems with a range of desirable properties not encountered in current methods

- Ordinary differential equations (ODE) for describing the system dynamics;
- A reduced set of generalized coordinates and a reduced set of model equations for fast evaluation;
- A constant reduced order basis.

These benefits are not encountered in previous system level model order reduction schemes for flexible multibody simulation, like the Global Modal Parameterization (GMP)[13]. The variable coordinate transformation encountered in GMP leads to complex inertial forces[14] and a relatively invasive model setup procedure. The proposed SLAP method, on the other hand, leads to a constant mass matrix and can be defined from easy-to-obtain simulation and flexible multibody data. The SLAP approach allows for the training-based reduction of arbitrary fixed topology flexible multibody models. A projection on the dominant system level modes is performed, which enables an exact or approximate constraint elimination, and selection of the main dynamics. This results in a small set of ODEs with a constant mass-matrix and nonlinear internal forces. The current approach is only intended to address small deformation problems as the main aim is to obtain an easy-to-set-up reduced order model with a model structure in a more favorable ODE form. In literature alternative methods have been presented which also account for large deformation effects[15,16,17,18] in flexible multibody simulation, and which are generally more intrusive with respect to the reference models.

The proposed method can be applied non-intrusively with respect to existing flexible multibody software. The method extracts the simulated motion of the bodies for (a range of) reference simulation(s) in order to construct a reduced order basis (ROB), as discussed in Sec. 2-3. Moreover, we discuss how this data-driven approach allows to construct a ROB which is consistent with the joint constraints, without the necessity to explicitly have access to these constraint equations. The method also extracts body mass and stiffness matrices from external finite-element software, as can be easily performed through the available interfaces in this software. From these body level contributions, the reduced order equations of motion for the SLAP model can be constructed, as discussed in Sec. 4. The result is a closed form reduced multibody description which can be exploited in a range of applications. This flow of information is summarized in Fig. 1 . The proposed methodology is validated numerically in Sec. 6. This validation demonstrates the fast convergence of the SLAP model for an increasing number of DOFs and also highlights the care which must be taken to avoid the addition of spurious rigid body modes.

2 | REFERENCE FLEXIBLE MULTIBODY MODEL AND TRAINING

In this work we consider flexible multibody models comprising only flexible bodies. In general, the differential algebraic equations (DAEs) describing the continuous time behavior of these models can be written as[19]:

$$\mathbf{M}(\mathbf{q})\ddot{\mathbf{q}} + \mathbf{f}^{\text{gyr}}(\mathbf{q},\dot{\mathbf{q}}) + \mathbf{f}^{\text{damp}}(\mathbf{q},\dot{\mathbf{q}}) + \mathbf{f}^{\text{int}}(\mathbf{q}) - \mathbf{C}(\mathbf{q})^T\lambda = \mathbf{f}^{\text{ext}}, \tag{1}$$

$$\mathbf{c}(\mathbf{q}) = \mathbf{0}. \tag{2}$$

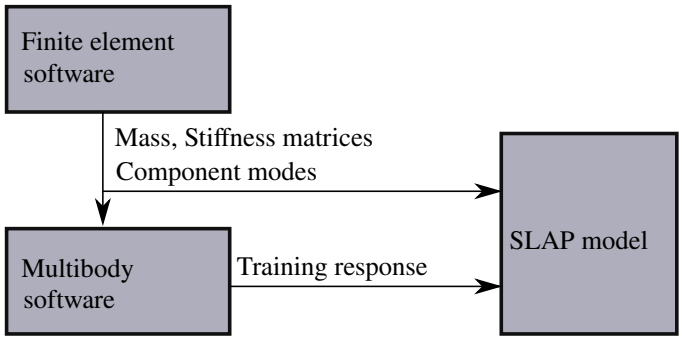

FIGURE 1 Method overview

In this system of equations the inertial forces are generally a nonlinear function of the generalized multibody coordinates $\mathbf{q}$ and their velocities $\dot{\mathbf{q}}$. Note that depending on the orginal multibody formulation the physical meaning of the generalized coordinates $\mathbf{q}$ varies. These inertial forces therefore consist of acceleration dependent terms and gyroscopic forces $\mathbf{f}^{\text{gyr}}$. Similarly the damping forces $\mathbf{f}^{\text{damp}}$ and internal elastic forces in the bodies $\mathbf{f}^{\text{int}}$ are also in general nonlinear functions of the generalized DOFs. For converting the model equations to an ODE form and from the point of view of model reduction, the nonlinear set of constraint equations $\mathbf{c}(\mathbf{q})$ (with Jacobian $\mathbf{C}(\mathbf{q})$) pose some specific difficulties. These constraints equations originate from two distinct sources:

- joint conditions between different bodies $\mathbf{c}^{joint}$;
- constraint equations present for particular motion parameterizations employed $\mathbf{c}^{par}$ (e.g. quaternions for rotational description).

The full constraint set can therefor be written as:

$$\mathbf{c} = \begin{bmatrix} \mathbf{c}^{joint} \\ \mathbf{c}^{par} \end{bmatrix}. \tag{3}$$

The elimination of these constraint equations through a projection of the equations of motion onto a system level reduction basis is discussed in Sec. 3.

The above equations cover a wide range of model descriptions, like the popular floating-frame-of-reference (FFR-CMS), where $\mathbf{q}$ consists of translational DOFs, rotational parameters and flexible participation factors, and the more recently introduced generalized component mode synthesis (GCMS) approach, where $\mathbf{q}$ consists of generalized participation factors. Small deformation flexible multibody simulation (almost) always starts from one of these component level reduced descriptions.

It is important to highlight that most commercial and research software for flexible multibody simulation, uses external finite element software or modules to set up a set of body reduced order bases Φ, typically based on Component Mode Synthesis [12], and to extract the underlying finite element mass $\mathbf{M}^{\text{FE}}$ and stiffness $\mathbf{K}^{\text{FE}}$ matrices for each body. This information is fed back to the multibody code in order to set up the equations of motion for the multibody model. In the proposed framework we exploit this external linking in order to also port this data to the model order reduction scheme.

A simulation of this original multibody model leads to the training response matrix $\mathbf{Q}^{tr}$:

$$\mathbf{Q}^{tr} = \begin{bmatrix} \mathbf{q}_1(t_1) & \dots & \mathbf{q}_1(t_{n^t}) \\ \vdots & \ddots & \vdots \\ \mathbf{q}_b(t_1) & \dots & \mathbf{q}_b(t_{n^t}) \end{bmatrix}, \tag{4}$$

for b bodies and n^t training timesteps, where the contribution from body i to a vector $\mathbf{a}$ is denoted as $\mathbf{a}_i$. Correspondingly the response can also be described for the full set of nodal coordinates for the different bodies over time as:

$$\mathbf{X}^{tr} = \begin{bmatrix} \mathbf{x}_1(t_1) & \dots & \mathbf{x}_1(t_{n^t}) \\ \vdots & \ddots & \vdots \\ \mathbf{x}_b(t_1) & \dots & \mathbf{x}_b(t_{n^t}) \end{bmatrix}, \tag{5}$$

where $\mathbf{x}_i$ are the nodal coordinates for the underlying FE mesh of body i. In most commercial and research flexible multibody software it is possible to extract these vectors and matrices of nodal coordinates for e.g. post-processing purposes. These nodal coordinates are used for the presented reduction framework, as this information is consistent over different original multibody

formulations. However, it is important to highlight that for the proposed framework, it is irrelevant whether these training simulations were performed using local or absolute coordinates, as long they can be post-processed into absolute nodal coordinates. It is this externally available information which will be exploited to perform the model order reduction setup. Together with the finite-element mass and stiffness matrices from the finite-element models of the bodies, this provides all the data required to set up the proposed system-level reduced order model. The training set should be sufficiently rich to capture the full relevant motion manifold. For specific problems, like chaotic systems, this could be difficult to achieve in practice and we consider a dedicated analysis of the proposed method for the case of chaotic systems beyond the scope of this work.

3 | REDUCED ORDER BASIS AND CONSTRAINT ELIMINATION

In this section we describe how the reduced order basis (ROB) selection for the system-level affine parameterization is performed. Specific focus is drawn on how an adequately chosen coordinate transformation can be exploited to allow an affine reduced description of the system level DOFs with (approximate) constraint elimination.

3.1 | Affine reduced order basis projection

The model order reduction proposed in this work is based on a constant reduced order basis $\mathbf{\Phi}^{\mathrm{sl}}$ which enables an affine approximation of the motion, accurately captures the main motion modes and inherently incorporates (an approximation of) the joint conditions in the multibody model. In this work we will develop an affine approximation which allows to describe the full nodal coordinates $\mathbf{x}$ through a constant system level ROB $\mathbf{\Phi}^{\mathrm{sl}}$, irregardless of the multibody formulation employed for the training model:

$$\mathbf{x} \approx \boldsymbol{\rho} + \mathbf{\Phi}^{\mathrm{sl}}\boldsymbol{\eta}, \tag{6}$$

$$\mathbf{c}(\boldsymbol{\rho} + \mathbf{\Phi}^{\mathrm{sl}}\boldsymbol{\eta}) \approx \mathbf{0}, \qquad \forall \quad \boldsymbol{\eta} \in \mathbb{R}^m, \tag{7}$$

where $\boldsymbol{\rho} \in \mathbb{R}^n$ is a reference configuration which complies with the constraints, $\mathbf{\Phi}^{\mathrm{sl}} \in \mathbb{R}^{n\times m}$ is the (constant) system level reduced order basis, and $\boldsymbol{\eta} \in \mathbb{R}^m$ are the reduced degrees-of-freedom. The approximate compliance with the constraints of the proposed affine parameterization is an important condition for the proposed reduction scheme. The definition of this constant ROB $\mathbf{\Phi}^{\mathrm{sl}}$ is the subject of the remainder of this section.

First the reference configuration $\boldsymbol{\rho}$ is selected. In this work we select the initial configuration from the training matrix:

$$\boldsymbol{\rho} = \mathbf{X}^{tr}(t_1), \tag{8}$$

and in practice any configuration which complies with the constraint equations could be selected. It is moreover interesting to highlight that this does not need to be an undeformed configuration. The particular choice of $\boldsymbol{\rho}$ is therefor not critical, even though as a rule of thumb it might be more convenient to use an undeformed configuration.

In order to obtain the ROB $\mathbf{\Phi}^{\mathrm{sl}}$, Proper Orthogonal Decomposition (POD) is employed [20]. This POD basis is obtained through a (thin) singular value decomposition on the training response data with the reference configuration eliminated $\boldsymbol{\rho}$:

$$\mathbf{W}\mathbf{\Sigma}\mathbf{V}^T = \mathrm{svd}\left(\mathbf{X}^{tr,\Delta}\right) = \mathrm{svd}\left(\left[\mathbf{X}^{tr}\left(t_2\right) - \boldsymbol{\rho},\ \ldots,\ \mathbf{X}^{tr}\left(t_n\right) - \boldsymbol{\rho}\right]\right), \tag{9}$$

and the system-level ROB $\mathbf{\Phi}^{\mathrm{sl}}$ is obtained by only retaining the m most dominant modes in $\mathbf{W}$:

$$\mathbf{\Phi}^{\mathrm{sl}} = \left[\mathbf{W}_{,1}, \ldots, \mathbf{W}_{,m}\right], \tag{10}$$

where the ith column of a matrix $\mathbf{A}$ is denoted by $\mathbf{A}_{,i}$. Section 3.3 describes how setting up the reduced order basis from the nodal DOFs $\mathbf{x}$ instead of the generalized multibody DOFs $\mathbf{q}$ allows to (approximately) eliminate the constraint equations through a constant ROB. Previous work on system-level model reduction for flexible multibody simulation through the Global Modal Parameterization (GMP) [13,14] required a configuration dependent reduced motion parameterization to eliminate the constraint equations. This aspect greatly complicates the reduced model description and limits the general applicability of GMP, as these parameterizations can be difficult to set up in practice.

3.2 | Training data compression

The above described direct reduction approach is generally applicable but will often pose practical issues due to the very large data sets obtained from flexible multibody models. This is due to the (very) large number of DOFs typically present for each FE body description (10k-100k nodes are common for most structural body FE models), multiplied by the number of bodies b for a considerable number of timesteps n^t. Directly performing the singular value decomposition is therefore often computationally intractable. For example performing the singular value decomposition in Matlab for a relatively small model with two bodies, each with 30000 DOFs for 1000 timesteps already requires over 30 gigabytes of RAM, which is at the limit for regular desktop systems. In this work we therefore propose an intermediate data compression which preserves the singular values but drastically lowers the number of DOFs on which the singular value decomposition is performed without any loss in accuracy for flexible multibody models. Alternatively, several methods have been proposed in general data compression literature, like gappy POD[21], randomized singular value decomposition[22], and hierarchical POD[23], to deal with identifying a low rank approximation of large datasets at a feasible computational load. However, these schemes do not explicitly exploit the underlying model structure and we expect the scheme proposed hereafter to lead to even smaller computational loads due to the very small number of retained coordinates.

This data compression is obtained from the observation that practical large scale small-deformation flexible multibody models already employ component-level model order reduction. Over the years a wide range of approaches have been proposed to express the body deformation in an approximate fashion, typically exploiting reduction approaches from linear structural dynamics[11,24]. This in turn implies that the motion of the full multibody system is inherently constrained to a lower dimensional manifold than the one for the full mesh. The proposed compression therefor starts from the local body-attached reduced order basis for body i employed in the reference multibody model $\mathbf{\Psi}_i^b$:

$$\mathbf{u}_i = \mathbf{u}_i^0 + \mathbf{\Psi}_i^b \mathbf{q}_i, \tag{11}$$

where $\mathbf{u}_i \in \mathbb{R}^{3n_i^n}$ are the nodal coordinates for body i expressed in a local body-attached reference frame with undeformed coordinates $\mathbf{u}_i^0 \in \mathbb{R}^{3n_i^n}$, reduced deformation modes $\mathbf{\Psi}^b \in \mathbb{R}^{3n_i^n \times m_i^b}$, and generalized body DOFs $\mathbf{q}_i \in \mathbb{R}^{m_i^b}$. The absolute coordinates expressed in the global reference frame for the nodes of a body i can then be generally obtained from:

$$\mathbf{x}_i = \tilde{\mathbf{I}}_i \mathbf{x}_i^t + \bar{\mathbf{R}} \left(\mathbf{u}_i^0 + \mathbf{\Psi}_i^b \mathbf{q}_i \right), \tag{12}$$

where in $\mathbf{x}_i^t \in \mathbb{R}^3$ denotes the body translation, $\tilde{\mathbf{I}}_t \in \mathbb{R}^{3n_i^n \times 3}$ is a translational project matrix consisting of vertically concatenated three-by-three unity matrices $\mathbf{I}$:

$$\tilde{\mathbf{I}} = \begin{bmatrix} \mathbf{I}^{3\times3} \\ \vdots \\ \mathbf{I}^{3\times3} \end{bmatrix}, \tag{13}$$

and $\bar{\mathbf{R}} \in \mathbb{R}^{3n_i^n \times 3n_i^n}$ is a body rotation consisting of a block diagonal stack of the three-by-three body rotation matrix $\mathbf{R}$ for all nodes:

$$\bar{\mathbf{R}} = \begin{bmatrix} \mathbf{R} & \mathbf{0} & \mathbf{0} \\ \mathbf{0} & \ddots & \mathbf{0} \\ \mathbf{0} & \mathbf{0} & \mathbf{R} \end{bmatrix}. \tag{14}$$

In the most general case, and without exploiting any additional information from the multibody system, the following holds:

- the reference body translation resides on a three-dimensional linear manifold spanned by $\tilde{\mathbf{I}}$.
- the rotation matrices $\mathbf{R}$ and $\bar{\mathbf{R}}$ normally resides on a nonlinear manifold, and this nonlinear manifold is a subspace of a general nine-dimensional manifold as:

$$\mathbf{R} = \begin{bmatrix} r^1 & r^4 & r^7 \\ r^2 & r^5 & r^8 \\ r^3 & r^6 & r^9 \end{bmatrix}, \tag{15}$$

$$= \sum_{k=1}^{9} \mathbf{I}^k r^k, \tag{16}$$

with a selection matrices $\mathbf{I}^k \in \mathbb{R}^{3\times3}$:

$$\mathbf{I}^1 = \begin{bmatrix} 1 & 0 & 0 \\ 0 & 0 & 0 \\ 0 & 0 & 0 \end{bmatrix}, \quad \mathbf{I}^2 = \begin{bmatrix} 0 & 0 & 0 \\ 1 & 0 & 0 \\ 0 & 0 & 0 \end{bmatrix}, \quad \mathbf{I}^3 = \begin{bmatrix} 0 & 0 & 0 \\ 0 & 0 & 0 \\ 1 & 0 & 0 \end{bmatrix}, \quad \mathbf{I}^4 = \begin{bmatrix} 0 & 1 & 0 \\ 0 & 0 & 0 \\ 0 & 0 & 0 \end{bmatrix}, \quad \mathbf{I}^5 = \begin{bmatrix} 0 & 0 & 0 \\ 0 & 1 & 0 \\ 0 & 0 & 0 \end{bmatrix}$$

$$\mathbf{I}^6 = \begin{bmatrix} 0 & 0 & 0 \\ 0 & 0 & 0 \\ 0 & 1 & 0 \end{bmatrix}, \quad \mathbf{I}^7 = \begin{bmatrix} 0 & 0 & 1 \\ 0 & 0 & 0 \\ 0 & 0 & 0 \end{bmatrix}, \quad \mathbf{I}^8 = \begin{bmatrix} 0 & 0 & 0 \\ 0 & 0 & 1 \\ 0 & 0 & 0 \end{bmatrix}, \quad \mathbf{I}^9 = \begin{bmatrix} 0 & 0 & 0 \\ 0 & 0 & 0 \\ 0 & 0 & 1 \end{bmatrix} \tag{17}$$

where r^k can take any value in $\mathbb{R}$, and similarly:

$$\bar{\mathbf{R}} = \sum_{k=1}^{9} \bar{\mathbf{I}}^k r^k, \tag{18}$$

where $\bar{I}^k$ is similarly defined to the block diagonal matrix $\bar{\mathbf{R}}$ from Eq. (14).

These conditions imply that the global nodal coordinates for body i need to reside on a linear global manifold spanned by:

$$\mathbf{x}_i \in \left[\tilde{\mathbf{I}}_t \mid \bar{\mathbf{I}}^1 \mathbf{u}_i^0, \ \ldots, \ \bar{\mathbf{I}}^9 \mathbf{u}_i^0 \mid \bar{\mathbf{I}}^1 \boldsymbol{\Psi}_i^b, \ \ldots, \ \bar{\mathbf{I}}^9 \boldsymbol{\Psi}_i^b\right] \tag{19}$$

An orthonormal basis $\boldsymbol{\Psi}_i^g$ in this span can be constructed from the different contributions in Eq. (19). At most this basis will have a rank of $3 + 9 + 9m_i^b (\ll 3n_i^n)$ for body i and is known as the Generalized Component Mode Synthesis basis[25,26].

If this basis $\boldsymbol{\Psi}_i^g$ is computed for each body i in the multibody model, a system level basis $\bar{\boldsymbol{\Psi}}^g$ can be set up:

$$\bar{\boldsymbol{\Psi}}^g = \begin{bmatrix} \boldsymbol{\Psi}_1^g & 0 & 0 \\ 0 & \ddots & 0 \\ 0 & 0 & \boldsymbol{\Psi}_b^g \end{bmatrix}. \tag{20}$$

As $\left(\boldsymbol{\Psi}_i^g\right)^T \boldsymbol{\Psi}_i^g = \mathbf{I}$, with the above definition it also holds that:

$$\left(\bar{\boldsymbol{\Psi}}^g\right)^T \bar{\boldsymbol{\Psi}}^g = \mathbf{I}. \tag{21}$$

As each of the constituent matrices $\boldsymbol{\Psi}_i^g$ span the full motion space for each body i, this basis $\bar{\boldsymbol{\Psi}}^g$ spans the full motion space of the multibody model where each body can move independently. This basis $\bar{\boldsymbol{\Psi}}^g$ can now be used to project the full system nodal responses onto a much smaller data set:

$$\hat{\mathbf{Q}}^{tr} = \left(\bar{\boldsymbol{\Psi}}^g\right)^T \mathbf{X}^{tr,\Delta}, \tag{22}$$

$$= \begin{bmatrix} \left(\boldsymbol{\Psi}_1^g\right)^T \mathbf{X}_1^{tr,\Delta} \\ \vdots \\ \left(\boldsymbol{\Psi}_b^g\right)^T \mathbf{X}_b^{tr,\Delta} \end{bmatrix}. \tag{23}$$

It is important to highlight that this transformation to $\hat{\mathbf{Q}}^{tr}$ retains the singular values of $\mathbf{X}^{tr}$, such that a meaningful order reduction with respect to the actual system motion can be performed. See Appendix A for a proof of the singular value preservation. This implies that any singular value based model order reduction strategy is equally valid on the intermediary reduced coordinates $\hat{\mathbf{Q}}^{tr}$ as on the original nodal coordinates $\mathbf{X}^{tr}$. Notice that clearly the same is not true when projecting onto FFR-CMS coordinates as this involves a strongly nonlinear transformation. Moreover, this also implies that any conclusions on using the singular value decomposition for constraint elimination in Sec. 3.3 are equally true for the intermediary projected coordinates $\hat{\mathbf{Q}}^{tr}$ as it is for the full global nodal coordinates $\mathbf{X}^{tr}$.

At this point a much smaller data set $\hat{\mathbf{Q}}^{tr}$ is available on which the singular value decomposition can be effectively performed to extract the reduced order basis:

$$\hat{\mathbf{W}}\Sigma\hat{\mathbf{V}} = \text{svd}\left(\hat{\mathbf{Q}}^{tr}\right). \tag{24}$$

When using this intermediate reduction, the reduced order basis is set up by truncating $\hat{\mathbf{W}}$ to the first m components, where $m < n - n^c$. For most applications, a clear decay in the singular values will be observed for an increasing mode number. The reduction basis for the GCMS coordinates projection is denoted as:

$$\hat{\mathbf{W}}^* = \left[\hat{\mathbf{W}}_{,1}, \ \ldots, \ \hat{\mathbf{W}}_{,m}\right], \tag{25}$$

and this basis can be transformed back to a reduced order basis for the full nodal coordinates:

$$\boldsymbol{\Phi}^{\text{sl}} = \bar{\boldsymbol{\Psi}}^g \hat{\mathbf{W}}^*, \tag{26}$$

with $\boldsymbol{\Phi}^{\text{sl}} \in \mathbb{R}^{n \times m}$. As the proposed intermediate data compression exactly preserves the singular values of the original data, this basis will be the same as the one from Eq. (10). This system level matrix can again be split up into contributions for the b bodies

for processing of the model matrices, as discussed in the Sec. 4:

$$\mathbf{\Phi}^{\mathrm{sl}} = \begin{bmatrix} \mathbf{\Phi}^{\mathrm{sl}}_1 \\ \vdots \\ \mathbf{\Phi}^{\mathrm{sl}}_b \end{bmatrix}. \tag{27}$$

This reduced order basis $\mathbf{\Phi}^{\mathrm{sl}}$, together with the reference configuration $\boldsymbol{\rho}$, will be exploited to set up the reduced equations of motion in the following sections.

3.3 | Constraint elimination through global system level reduced order basis

In this section we explain how an affine coordinate projection on the nodal coordinates $\mathbf{x}$ can be exploited to perform an (approximate) constraint elimination, and why this is not generally possible when operating directly on the generalized multibody DOFs $\mathbf{q}$ (as had been proposed in previous work [13]).

In this work, the considered systems have a fixed topology. For fixed topology the joints are constantly active between the same nodal pairs during the course of the motion. This covers many common joints in mechanical systems like spherical, revolute and universal joints, but excludes others like sliding joints between two flexible bodies or contacts.

As discussed before, two types of constraints are typically encountered in flexible multibody simulation: joint constraints $\mathbf{c}^{joint} \in \mathbb{R}^{n^c}$ and parameterization constraints $\mathbf{c}^{par}$. The parameterization constraints $\mathbf{c}^{par}$ are inherently tied to the choice of generalized coordinates $\mathbf{q}$, e.g. to the rotational parameterization. For the proposed reduction scheme these are inherently eliminated as after the reference simulation, all evaluations occur on a global nodal coordinate level, and these constraint equations are therefore omitted from the remainder of the discussion in this section.

The second type of constraints, due to the joints between different bodies, however poses some specific difficulties. In general the joint constraint equations can be eliminated from the equations of motion, by restricting the motion of the system to the kernel $\mathbf{N}$ of the Jacobian of the constraint equations $\mathbf{C} \in \mathbb{R}^{(n^c \times n}$. For any given training set $\mathbf{X}^{tr}$, this condition can be evaluated for all constraint Jacobians evaluated for the training data $\mathbf{C}^{tr} \in \mathbb{R}^{(n^c \cdot n^t) \times n}$ such that:

$$\mathbf{N} = \ker\left(\mathbf{C}^{tr}\right) = \ker\left(\begin{bmatrix} \mathbf{C}(\mathbf{x}(t_1)) \\ \vdots \\ \mathbf{C}(\mathbf{x}(t_{n^t})) \end{bmatrix}\right) \quad \text{such that} \quad \mathbf{C}^{tr}\mathbf{N} = \mathbf{0}, \tag{28}$$

with

$$\mathbf{C}(\mathbf{x}) = \frac{\partial \mathbf{c}(\mathbf{x})}{\partial \mathbf{x}}. \tag{29}$$

This implies that $\mathbf{\Phi}^{\mathrm{sl}} \in \mathrm{span}(\mathbf{N})$, as in this case:

$$\left(\mathbf{\Phi}^{\mathrm{sl}}\right)^T \mathbf{C}(\mathbf{x})^T = \mathbf{0}, \qquad \forall \quad \mathbf{x} \in \mathbf{X}^{tr}, \tag{30}$$

and the constraint equations can be (approximately) eliminated from the equations of motion. However, in this work, contrary to previous works [27,28], the null-space of the constraints is not explicitly computed to set up the reduced order model, but is implicitly accounted for through the singular value decomposition on the training data. In the following paragraphs the cases of linear and nonlinear joint constraint equations are discussed.

In this work we consider the case of linear joint constraint equations as a function of the nodal coordinates $\mathbf{x}$. Linear joint constraint equations are obtained for example for a nodal coordinate description in the case of spherical joints between node pairs of the different bodies, which can be practically exploited to set up the models for a range of mechanisms [28].

A set of linear constraint equations can be written as:

$$\mathbf{c}(\mathbf{x}) = \mathbf{c}^0 + \mathbf{C}\mathbf{x} = \mathbf{0}, \tag{31}$$

with the constraints $\mathbf{c}(\mathbf{x}) \in \mathbb{R}^{n^c}$, a constant offset term $\mathbf{c}^0 \in \mathbb{R}^{n^c}$ and a constant matrix $\mathbf{C} \in \mathbb{R}^{n^c \times n}$. As discussed in the previous section, a reference configuration $\boldsymbol{\rho}$ is first selected which meets the joint constraint equations:

$$\mathbf{c}_0 + \mathbf{C}\boldsymbol{\rho} = \mathbf{0}. \tag{32}$$

From the definition of the remaining training data $\mathbf{X}^{tr,\Delta}$ in Eq. (9), it is clear that this will lie in the constraint kernel as all training data must comply with the constraints:

$$\begin{aligned}\mathbf{0} &= \mathbf{c}_0 + \mathbf{C}\mathbf{X}^{tr}_{,i} = \mathbf{c}_0 + \mathbf{C}\cdot\left(\boldsymbol{\rho} + \mathbf{X}^{tr,\Delta}_{,i}\right)\\ &= \mathbf{c}_0 + \mathbf{C}\boldsymbol{\rho} + \mathbf{C}\mathbf{X}^{tr,\Delta}_{,i} = \mathbf{C}\mathbf{X}^{tr,\Delta}_{,i} = \mathbf{0} \quad \forall i = \{1,\dots,n^t\}.\end{aligned} \tag{33}$$

Notice that the presence of $\boldsymbol{\rho}$ is essential as otherwise e.g. $\eta = \mathbf{0}$ would not comply with the constraints in Eq (32). The remaining training data should therefore lie in the kernel of the constraint Jacobian. This can be written as:

$$\mathbf{X}^{tr,\Delta} = \mathbf{N}\mathbf{x}^{ce} + \mathbf{C}^T 0, \tag{34}$$

with $\mathbf{x}^{ce} \in \mathbb{R}^{n-n^c}$ a set of minimal coordinates. The singular value decomposition for a generally random set of admissible coordinates can then be written as:

$$\text{svd}(\mathbf{X}^{tr,\Delta}) = \begin{bmatrix}\text{orth}(\mathbf{N}) & \text{orth}(\mathbf{C}^T)\end{bmatrix}\begin{bmatrix}\boldsymbol{\Sigma} & \mathbf{0}\\ \mathbf{0} & \mathbf{0}\end{bmatrix}\mathbf{V}^T, \tag{35}$$

where $\boldsymbol{\Sigma} \in \mathbb{R}^{(n-n^c)\times(n-n^c)}$ is a diagonal matrix with non-zero singular values, and $\text{orth}(\mathbf{A})$ denotes the orthonormalization of a matrix $\mathbf{A}$:

$$\text{orth}(\mathbf{A})^T\text{orth}(\mathbf{A}) = \mathbf{I} \quad \text{where} \quad \text{orth}(\mathbf{A}) \in \text{span}(\mathbf{A}). \tag{36}$$

Performing the truncation on this singular value decomposition, as discussed in Sec. 3.1, rejects any contributions in the span of the constraint equations and therefor effectively enables an exact constraint elimination.

Clearly it is of large benefit if the model joint constraints are indeed linear from a model order reduction perspective, as these joints can be exactly represented. However, as mentioned before, for generalized coordinates $\mathbf{q}$ in FMBS, the structure of the constraint equations depends on the choice of coordinates. For example, linear constraint equations for spherical joints in nodal coordinates are described by nonlinear equations in FFR-CMS coordinates, which highlights the necessity of converting back to nodal coordinates to perform the model order reduction.

To apply the proposed reduction scheme, converting as many joint constraints to spherical joints has an significant advantage for obtaining an accurate reduced order model, as these joints are described through linear equations in the global nodal coordinates. However, in general also nonlinear joint constraints will be present in most models (e.g. revolute joints), which makes an exact affine elimination, as discussed in the previous paragraph, infeasible. It is therefore important to highlight that the proposed approach might be capable of approximately capturing these constraints, but this cannot be guaranteed. For applications where these joints are present, a potential solution is therefore to replace them by a set of *equivalent* linear nodal constraints in the reference model, e.g. two spherical joints on colinear nodes instead of a revolute joint. The treatment of more general nonlinear joint constraint is a topic of future research and out of the scope of the current work.

4 | REDUCED EQUATIONS OF MOTION

For the derivation of the equations of motion for the proposed reduced order model, the starting point is the Lagrangian of the system expressed as a function of the system-level reduced DOFs $\boldsymbol{\eta}$:

$$\mathcal{L}(\boldsymbol{\eta}, t) = \mathcal{K}(\boldsymbol{\eta}, \dot{\boldsymbol{\eta}}) - \mathcal{V}(\boldsymbol{\eta}), \tag{37}$$

wherein the kinetic energy $\mathcal{K}$ will lead to the generalized inertial forces, the internal energy $\mathcal{V}$ to the generalized internal elastic forces. Note that there are no constraints present in the Lagrangian Eq. (37) as these are assumed approximately eliminated through the system-level reduced coordinates. Hamilton's principle is applied on this Lagrangian to obtain the reduced generalized forces:

$$\frac{d}{dt}\left(\frac{\partial \mathcal{L}}{\partial \dot{\boldsymbol{\eta}}}\right) - \frac{\partial \mathcal{L}}{\partial \boldsymbol{\eta}} = \mathbf{g}^{\text{np}}, \tag{38}$$

with the $\mathbf{g}^{\text{np}}$ representing the generalized non-potential forces like damping $\mathbf{g}^{\text{damp}}$ and external forces $\mathbf{g}^{\text{ext}}$, to obtain the equations of motion. This leads to the time-continuous ordinary differential equations (ODE) of motion due to the approximate elimination of the constraints (as discussed in Sec. 3.3):

$$\mathbf{g}^{\text{iner}}(\eta, \ddot{\boldsymbol{\eta}}) + \mathbf{g}^{\text{damp}}(\dot{\boldsymbol{\eta}}) + \mathbf{g}^{\text{int}}(\boldsymbol{\eta}) = \mathbf{g}^{\text{ext}}, \tag{39}$$

with $\mathbf{g}^{\text{iner}}$ and $\mathbf{g}^{\text{int}}$ respectively the generalized inertial and internal elastic forces. This ODE structure is highly valuable in a range of applications and is difficult to obtain reliably with a general FMBS description. The different generalized force contributions in Eq. (39) are discussed in the following subsections.

4.1 | Inertial forces

For evaluating the kinetic energy of a body, the velocities of all nodes are projected onto a body-attached frame, as this allows to use the original FE lumped mass matrix. The velocity $\mathbf{v}_{ij} \in \mathbb{R}^3$ of a node j in a body i projected onto a body-attached frame can be written as:

$$\mathbf{v}_{ij} = \mathbf{R}_i \mathbf{\Phi}^{\text{sl}}_{ij} \dot{\boldsymbol{\eta}}, \tag{40}$$

where $\mathbf{R}_i \in \mathbb{R}^{3\times3}$ is a body-attached rotation matrix, and $\mathbf{\Phi}^{\text{sl}}_{ij} \in \mathbb{R}^{3\times m}$ represents the reduced order basis for a node j on a body i.

For the inertial forces we assume a mass-matrix $\mathbf{M}^{\text{FE}}$ with only displacement contributions for the finite element models for all bodies (i.e. lumped mass matrices or solid finite elements) [19]. For a node j on body i, the contribution to the mass matrix can be written as:

$$\mathbf{M}^{\text{FE}}_{ij} = m_{ij} \mathbf{I}^{3\times3}, \tag{41}$$

where the full mass matrix for body i is a block-diagonal matrix with the entries for the different nodes on its diagonal. By using Eq. (40), the kinetic energy in the reduced coordinates can be written as:

$$\mathcal{K} = \frac{1}{2} \sum_{i=1}^{b} \sum_{j=1}^{n_i^n} \left(\mathbf{R}_i \mathbf{\Phi}^{\text{sl}}_{ij} \dot{\boldsymbol{\eta}} \right)^T \mathbf{M}^{\text{FE}}_{ij} \mathbf{R}_i \mathbf{\Phi}^{\text{sl}}_{ij} \dot{\boldsymbol{\eta}}, \tag{42}$$

$$= \frac{1}{2} \sum_{i=1}^{b} \sum_{j=1}^{n_i^n} \left(\mathbf{\Phi}^{\text{sl}}_{ij} \dot{\boldsymbol{\eta}} \right)^T m_{ij} \mathbf{R}_i^T \mathbf{R}_i \mathbf{\Phi}^{\text{sl}}_{ij} \dot{\boldsymbol{\eta}}, \tag{43}$$

$$= \frac{1}{2} \sum_{i=1}^{b} \sum_{j=1}^{n_i^n} \left(\mathbf{\Phi}^{\text{sl}}_{ij} \dot{\boldsymbol{\eta}} \right)^T \mathbf{M}^{\text{FE}}_{ij} \mathbf{\Phi}^{\text{sl}}_{ij} \dot{\boldsymbol{\eta}}, \tag{44}$$

with n_i^n the number of nodes for body i. The system-level mass-matrix $\mathbf{M}^{\text{sl}}$ for the system-level reduced model can then be constructed as:

$$\mathbf{M}^{\text{sl}} = \sum_{i=1}^{b} \left(\mathbf{\Phi}^{\text{sl}}_{i} \right)^T \mathbf{M}^{\text{FE}}_{i} \mathbf{\Phi}^{\text{sl}}_{i}, \tag{45}$$

and the generalized inertial forces $\mathbf{g}^{\text{iner}}$ can be evaluated as:

$$\mathbf{g}^{\text{iner}}(\ddot{\boldsymbol{\eta}}) = \mathbf{M}^{\text{sl}} \ddot{\boldsymbol{\eta}}. \tag{46}$$

This leads to a description with a constant (configuration independent) mass-matrix without the need to include gyroscopic forces. Notice that it is not necessary to explicitly account for contributions from the body rotation in the kinetic energy and inertial forces, as the SLAP scheme does not distinguish between translational and rotational motion as they are equally captured in the system-level modes. As discussed in the introduction, the mass matrix $\mathbf{M}^{\text{FE}}$ is obtained through the commonly available interfaces with finite element software and does not require any interaction with the reference flexible multibody code.

4.2 | Damping forces

In this work we consider only mass-proportional damping, other types of damping are not treated here for the sake of brevity. For a damping factor $\zeta \geq 0$, the generalized damping forces $\mathbf{g}^{\text{damp}}$ can be straightforwardly obtained from Eq. (46):

$$\mathbf{g}^{\text{damp}} = \zeta \mathbf{M}^{\text{sl}} \dot{\boldsymbol{\eta}}. \tag{47}$$

4.3 | Internal elastic forces

In order to evaluate the internal elastic energy, the node deformation is required. The local nodal deformation $\mathbf{d}_{ij} \in \mathbb{R}^3$ for node j on body i expressed in a body-attached frame, described by a translation $\mathbf{x}_i^t \in \mathbb{R}^3$ and a rotation matrix $\mathbf{R}_i \in \mathbb{R}^{3\times3}$, is given by:

$$\mathbf{d}_{ij} = \mathbf{R}_i (\boldsymbol{\rho}_{ij} + \mathbf{\Phi}^{\text{sl}}_{ij} \boldsymbol{\eta} - \mathbf{x}_i^t) - \mathbf{u}^0_{ij}, \tag{48}$$

with $\mathbf{u}_{ij}^0 \in \mathbb{R}^3$ the local reference undeformed nodal coordinates of node j in the body attached frame of body i.

Different methods can be defined for determining the reference translation $\mathbf{x}_i^t$ and rotation $\mathbf{R}_i$ for a body i. Ideally these two quantities are determined in a coupled fashion to minimize the internal energy. However, this leads to a relatively complex problem to solve iteratively. In this work we therefore propose a more pragmatic approach where:

- The reference translation for a body $\mathbf{x}_i^t$ is determined as the average translation of all n_i^n nodes j of a body i:

$$\mathbf{x}_i^t = \frac{1}{n_i^n} \sum_{j=1}^{n_i^n} \mathbf{x}_{ij} - \mathbf{x}_{ij}^0, \tag{49}$$

  and using an initially centered mesh, this can be written as:

$$\mathbf{x}_i^t = \frac{1}{n_i^n} \sum_{j=1}^{n_i^n} \mathbf{x}_{ij} = \boldsymbol{\rho}_i^t + \boldsymbol{\Phi}_i^{\mathrm{sl,t}} \boldsymbol{\eta}, \tag{50}$$

  where $\boldsymbol{\rho}^t \in \mathbb{R}^{(3b)}$ is the reference translated position for the b bodies and $\boldsymbol{\Phi}^{\mathrm{sl,t}} \in \mathbb{R}^{(3b)\times m}$ is the average translational component corresponding to the different motion modes. Taking these corrections into account Eq. (48) can be rewritten as:

$$\mathbf{d}_{ij} = \mathbf{R}_i(\boldsymbol{\rho}_{ij}^c + \boldsymbol{\Phi}_{ij}^{\mathrm{sl,c}} \boldsymbol{\eta}) - \mathbf{u}_{ij}^0, \tag{51}$$

- The rotation matrix $\mathbf{R}_i$ is defined to minimize the nodal displacements after correction for the reference translation $\mathbf{x}_i^t$:

$$\min_{\mathbf{R}_i \in \mathbb{R}^{3\times3}} \sum_{j=1}^{n_i^n} \|\mathbf{R}_i(\boldsymbol{\rho}_{ij}^c + \boldsymbol{\Phi}_{ij}^{\mathrm{sl,c}} \boldsymbol{\eta}) - \mathbf{x}_{ij}^0\|_2 \quad \text{s.t.} \quad \mathbf{R}_i^T \mathbf{R}_i = \mathbf{I}_{3\times3}. \tag{52}$$

  Using quaternions to describe the rotation, this optimisation problem can be converted to a simple four-by-four eigenvalue problem as discussed in in Appendix B. Using the previously defined $\boldsymbol{\Phi}^{\mathrm{sl,c}}$ to evaluate the nodal position, this problem can moreover be written as a direct function of the reduced coordinates $\boldsymbol{\eta}$, such that the computational load becomes independent of the original model size.

The different nodal deformations for the bodies can be grouped in a deformation vector for body i as:

$$\mathbf{d}_i = \begin{bmatrix} \mathbf{d}_{i1} \\ \vdots \\ \mathbf{d}_{in_i^n} \end{bmatrix}. \tag{53}$$

The internal elastic energy starting from the finite-element stiffness matrix $\mathbf{K}_i^{\mathrm{FE}}$ for body i can then be written as:

$$\mathcal{V}_i = \frac{1}{2} \sum_{i=1}^{b} \left(\mathbf{d}_i(\eta)\right)^T \mathbf{K}_i^{\mathrm{FE}} \mathbf{d}_i(\eta). \tag{54}$$

A straightforward implementation would imply evaluating all nodal coordinates for each body, which would lead to large computational loads. In order to circumvent this issue, we propose the use of a number of stiffness invariants. The definition of these invariants is based on a decomposition of the rotation matrix into its nine elements, as presented in Eqs.(15)-(18). Using this decomposition for the rotation matrix together with a block-diagonal matrix definition:

$$\bar{\mathbf{R}}_i = \begin{bmatrix} \mathbf{R}_i & \dots & \mathbf{0} \\ \vdots & \ddots & \vdots \\ \mathbf{0} & \dots & \mathbf{R}_i \end{bmatrix}, \tag{55}$$

the deformation for body i can be written as:

$$\mathbf{d}_i = \bar{\mathbf{R}}_i(\boldsymbol{\rho}_i^c + \boldsymbol{\Phi}_i^{\mathrm{sl,c}} \boldsymbol{\eta}) - \mathbf{x}_i^0 = \sum_{k=1}^{9} \bar{\mathbf{I}}^k (\boldsymbol{\rho}_i^c + \boldsymbol{\Phi}_i^{\mathrm{sl,c}} \boldsymbol{\eta}) r_i^k - \mathbf{x}_i^0. \tag{56}$$

Inserting this in Eq. (54) leads to the definition of the stiffness invariants for body i:

$$\mathcal{V}_i = \frac{1}{2}\left(\sum_{k=1}^{9} \bar{\mathbf{I}}^k(\boldsymbol{\rho}_i^c + \boldsymbol{\Phi}_i^{\mathrm{sl,c}}\boldsymbol{\eta})r_i^k - \mathbf{x}_i^0\right)^T \mathbf{K}^{\mathrm{FE}}\left(\sum_{l=1}^{9} \bar{\mathbf{I}}^k(\boldsymbol{\rho}_i^c + \boldsymbol{\Phi}_i^{\mathrm{sl,c}}\boldsymbol{\eta})r_i^l - \mathbf{x}_i^0\right), \tag{57}$$

$$= \frac{1}{2}\left(\mathbf{K}_i^{00} + 2\sum_{k=1}^{9}\left(\boldsymbol{\eta}^T\mathbf{K}_{ik}^{\eta 0} + \mathbf{K}_{ik}^{\rho^c 0}\right)r_i^k + \sum_{k,l=1}^{9}\left(\boldsymbol{\eta}^T\mathbf{K}_{ikl}^{\eta\eta}\boldsymbol{\eta} + \boldsymbol{\eta}^T\mathbf{K}_{ikl}^{\eta\rho}\right)r_i^k r_i^l\right), \tag{58}$$

with the stiffness invariants:

$$\mathbf{K}_i^{00} = \left(\mathbf{x}_i^0\right)^T \mathbf{K}_i^{\mathrm{FE}}\mathbf{x}_i^0, \quad \mathbf{K}_i^{00} \in \mathbb{R}^{1\times 1}, \tag{59}$$

$$\mathbf{K}_{ik}^{\eta 0} = \left(\bar{\mathbf{I}}^k\boldsymbol{\Phi}_i^{\mathrm{sl,c}}\right)^T \mathbf{K}_i^{\mathrm{FE}}\mathbf{x}_i^0, \quad \mathbf{K}_{ik}^{\eta 0} \in \mathbb{R}^{m\times 1}, \tag{60}$$

$$\mathbf{K}_{ik}^{\rho 0} = \left(\bar{\mathbf{I}}^k\boldsymbol{\rho}_i^c\right)^T \mathbf{K}_i^{\mathrm{FE}}\mathbf{x}_i^0, \quad \mathbf{K}_{ik}^{\rho 0} \in \mathbb{R}^{1\times 1}, \tag{61}$$

$$\mathbf{K}_{ikl}^{\eta\eta} = \left(\bar{\mathbf{I}}^k\boldsymbol{\Phi}_i^{\mathrm{sl,c}}\right)^T \mathbf{K}_i^{\mathrm{FE}}\left(\bar{\mathbf{I}}^l\boldsymbol{\Phi}_i^{\mathrm{sl,c}}\right), \quad \mathbf{K}_{ikl}^{\eta\eta} \in \mathbb{R}^{m\times m}, \tag{62}$$

$$\mathbf{K}_{ikl}^{\eta\rho} = \left(\bar{\mathbf{I}}^k\boldsymbol{\Phi}_i^{\mathrm{sl,c}}\right)^T \mathbf{K}_i^{\mathrm{FE}}\left(\bar{\mathbf{I}}^l\boldsymbol{\rho}_i^c\right), \quad \mathbf{K}_{ikl}^{\eta\rho} \in \mathbb{R}^{m\times 1}. \tag{63}$$

These stiffness invariants need to be evaluated during the reduced order model setup, and lead to an online computational load independent of the original model size and only dependent on the reduced model size m.

The system-level internal elastic energy is then obtained through summation of the contributions of all b bodies:

$$\mathcal{V} = \sum_{i=1}^{b} \mathcal{V}_i. \tag{64}$$

From this expression, the generalized internal forces expressed for the system level reduced coordinates can be evaluated as:

$$\mathbf{g}^{\mathrm{int}} = \frac{\partial \mathcal{V}}{\partial \boldsymbol{\eta}}, \tag{65}$$

$$= \sum_{i=1}^{b}\sum_{k=1}^{9}\left(\mathbf{K}_{ik}^{\eta 0}r_i^k + \left(\frac{\partial r_i^k}{\partial \boldsymbol{\eta}}\right)^T\left(\boldsymbol{\eta}^T\mathbf{K}_{ik}^{\eta 0} + \mathbf{K}_{ik}^{\rho 0}\right)^T\right) + \sum_{i=1}^{b}\sum_{k,l=1}^{9}\left(\mathbf{K}_{ikl}^{\eta\eta}\boldsymbol{\eta} + \frac{1}{2}\mathbf{K}_{ikl}^{\eta\rho}\right)r_i^k r_i^l + \sum_{i=1}^{b}\sum_{k,l=1}^{9}\left(\boldsymbol{\eta}^T\mathbf{K}_{ikl}^{\eta\eta}\boldsymbol{\eta} + \boldsymbol{\eta}^T\mathbf{K}_{ikl}^{\eta\rho}\right)\left(\frac{\partial r_i^k}{\partial \boldsymbol{\eta}}r_i^l + r_i^k\frac{\partial r_i^l}{\partial \boldsymbol{\eta}}\right)^T. \tag{66}$$

The evaluation cost of these generalized internal forces depends only on the number of bodies and the reduced order size of the system model.

When required for time-integration purposes (i.e. for implicit time integration), the generalized stiffness matrix for the SLAP model can be derived by differentiating these internal forces Eq. (66) with respect to the generalized reduced DOFs $\boldsymbol{\eta}$. As this is a straightforward exercise given the above equations, it is omitted here for the sake of brevity.

4.4 | External forces

The generalized global external forces $\mathbf{g}^{\mathrm{ext}}$ are also obtained from performing a Galerkin projection on the reduced order basis:

$$\mathbf{g}^{\mathrm{ext}} = \left(\boldsymbol{\Phi}^{\mathrm{sl}}\right)^T\mathbf{f}^{\mathrm{ext}}. \tag{67}$$

At this point we only consider global external forces. Future developments will focus on effective descriptions for other load types like torques and loads acting between different bodies.

4.5 | Equations of motion overview

Using the above defined forces, the equations of motion can be summarized as a set of nonlinear ordinary differential equations:

$$\mathbf{M}^{\mathrm{sl}}\ddot{\boldsymbol{\eta}} + \zeta\mathbf{M}^{\mathrm{sl}}\dot{\boldsymbol{\eta}} + \mathbf{g}^{\mathrm{int}}(\boldsymbol{\eta}) = \left(\boldsymbol{\Phi}^{\mathrm{sl}}\right)^T \mathbf{f}^{\mathrm{ext}}. \tag{68}$$

This description is similar to the one obtained for the GCMS model description proposed by Gerstmayr *et al.* [3], in that a constant mass-matrix is obtained in exchange for nonlinear internal forces. It is moreover interesting to notice that in contrast to the GMP approach [27] where a sampling needs to be performed for all force gradients, which is rather exhaustive and intrusive in the multibody code, to evaluate the reduced model forces, here an analytic expression is obtained solely based on the reduced model kinematics and original body FE matrices.

An additional hyper-reduction stage could be considered for reducing the evaluation cost in Eq. (66). Here a sparse sampling and weighting method like the ECSW-approach [29] could be employed to limit the number of contributing bodies to the internal force. However this aspect is not investigated further in this work as for FMBS the number of bodies is expected to be limited with respect to the number of reduced DOFs, such that this additional hyper-reduction is expected to only yield a limited computational cost reduction. However, future research will focus on further hyper-reduction of these models.

5 | PRACTICAL IMPLEMENTATION OF THE SLAP MODEL

In order to clarify the full workflow of setting up and running the SLAP model in a simulation, this section summarizes the different steps required and relates back to the relevant equations from the previous sections.

5.1 | SLAP model setup

The first stage in the SLAP setup process, is the definition of an adequate set of training simulations. Several key criteria should be considered:

- The motion of the mechanism should span a sufficient portion of the undeformed motion space in order to assure an accurate extraction of the rigid body modes. Notice that it is not necessary to have visited all possible configurations in order to describe them effectively, as will be demonstrated in Sec. 6.3.
- Forces (preferably uncorrelated) should be applied to all locations on which external forces are exerted. The magnitude of the applied forces should be similar to the expected magnitude of the loads during the SLAP simulation. Similarly, the dynamic content should be similar.

The training data can be obtained from a single long-term simulation which combines all relevant excitation cases after which $\mathbf{X}^{tr}$ is extracted, or can alternatively be obtained from parallel short-term simulations which each capture a portion of the relevant excitation. In the latter case, $\mathbf{X}^{tr}$ is obtained by concatenating the results from the parallel simulations.

Next the kinematic relations for the SLAP model can be extracted. First of all a reference configuration $\boldsymbol{\rho}$ needs to be selected. This can be any (preferably undeformed) configuration of the system. In practice this will often be the first assembled configuration in the simulation. From this $\mathbf{X}^{tr,\Delta}$ can be set up. Next the ROB $\boldsymbol{\Phi}^{\mathrm{sl}}$ needs to be constructed, where two different schemes can be pursued depending on the models size:

- For relatively small models (up to 1000 nodes in total), $\boldsymbol{\Phi}^{\mathrm{sl}}$ can be directly extracted from a singular value decomposition on $\mathbf{X}^{tr,\Delta}$, as described in Eqs. (9)-(10).
- For larger models, it will be advisable to first perform the training data compression as discussed in Sec. 3.2. This requires the extraction of the initial body level modes $\boldsymbol{\Psi}_i^b$ from the finite-element interface typically employed for flexible multibody model initialization. This can for example be through the modal neutral file (mnf) standard interface [12]. The resulting SLAP modes can then be obtained through the setup of $\bar{\boldsymbol{\Psi}}^g$ as defined in Eqs. (19)-(20), the evaluation of the compressed data $\hat{\mathbf{Q}}^{tr}$ in Eq. (23), and the evaluation of the SVD and back-projection to $\boldsymbol{\Phi}^{\mathrm{sl}}$ through Eqs. (24)-(26) .

An important parameter which needs to be selected is the number of retained system level modes m in the final ROB. As a general rule of thumb the decay of the singular values can be considered to perform a first selection. However, as will be demonstrated in the numerical validation in Sec. 6, due to the finite tolerance with which the joint constraints are met, the SVD

will pick up spurious rigid body modes when m is choosen too high. In order to ensure that m is not chosen too high in order for this two occur, two possibilities exist:

- Run a reconstructive simulation with the generated SLAP model to ensure no additional rigid body motion starts to occur.
- Evaluate the linearized eigenfrequencies of the SLAP model at the initial configuration in order to ensure that not too many (close-to-)rigid body modes are present in the model.

Finally, the SLAP mass matrix and stiffness invariants need to be set up. From the computed system level modes $\mathbf{\Phi}^{\text{sl}}$ and their respective split in the body contributions according to Eq. (27), this is achieved by evaluating Eq. (45) for the mass matrix, and Eqs. (59)-(63) for the stiffness invariants. The body level finite-element mass and stiffness matrices can again be extracted from common finite-element toolbox interfaces. Depending on the formulation employed to extract the body attached rotation matrix, some rotation invariants need to be computed as well. For the approach presented in this work, and outlined in detail in App. B, the rotation invariants as defined in Eq. (B21)-(B22) need to be set up as well.

5.2 | Online SLAP evaluation

During the simulation of the SLAP model, the generated invariants can be exploited in order to ensure that no evaluations which scale with the size of the original model are still required. An important benefit of the proposed SLAP scheme is the possibility to use standard explicit integrators which are only suitable for ODE models. In general, any integrator will require for each timestep:

- The evaluation of the inertial forces $\mathbf{g}^{\text{iner}}(\ddot{\boldsymbol{\eta}})$ is done through Eq. (46). As this is a simple matrix-vector multiplication of the SLAP model size m, it has a complexity of $\mathcal{O}(m^2)$.
- In the case of mass-proportional damping, the inertial force vector $\mathbf{g}^{\text{iner}}(\ddot{\boldsymbol{\eta}})$ can be reused, such that the complexity is only of $\mathcal{O}(m)$.
- The internal elastic forces $\mathbf{g}^{\text{int}}(\boldsymbol{\eta})$ for the SLAP model are obtained through Eq. (66). Different schemes can be employed to evaluate the body attached rotation matrix element, and in this work we propose to evaluate these from the eigenvalue problem of Eq. (B25) and Eq. (B17). The required derivatives of the rotation matrix elements with respect to the reduced DOFs are obtained from Eq. (B26) and the corresponding derivatives in the quaternion based rotation matrix. For computational complexity, it is interesting to note that the overall cost of these rotation matrix and derivative evaluations only scale with $\mathcal{O}(bm)$, as the problem to solve is always a four-dimensional eigenvalue problem. The largest cost will therefore lie in evaluating the different matrix-vector products with the stiffness invariants, which will scale with $\mathcal{O}(bm^2)$. However, as m should be sufficiently small, this computational load should also remain limited. However, the final evaluation cost does remain dependent on the number of bodies, but their respective size is irrelevant.

In the case of an implicit simulation, the Jacobians for these forces also need to be evaluated. For the inertial and mass-proportional damping terms these are readily available. For the internal elastic forces on the other hand these are more involved, and for the sake of brevity we do not expand these terms here in detail. Finally, the obtained SLAP responses will need to be transformed back to the full order model domain for further post-processing purposes. This implies the simple matrix-vector product:

$$\mathbf{x}^{SLAP} = \boldsymbol{\rho} + \mathbf{\Phi}^{\text{sl}}\eta. \tag{69}$$

From the above outlined procedure the SLAP simulation can be performed and the results can be post-processed.

6 | VALIDATION

This section considers a numerical validation of the proposed reduction approach. The considered case is a flexible four bar mechanism. First the case definition is described and next several aspects of the SLAP model are investigated. All validations have been conducted in an in-house multibody research code implemented in Matlab[30].

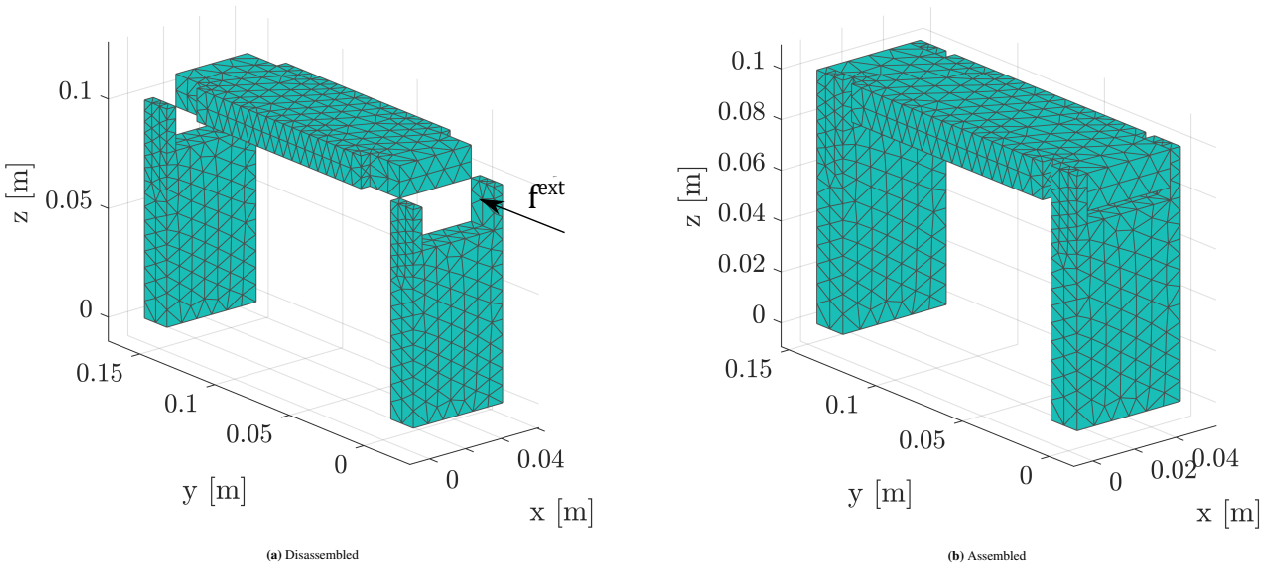

(a) Disassembled **(b)** Assembled

FIGURE 2 Flexible four-bar mechanism

6.1 | Model description

For the validation of the proposed approach, a four bar mechanism is used as shown in Fig. 2 . The finite element models for the three linear elastic flexible components are constructed with a tetrahedron mesh in Nastran[12]. The properties of each body are shown in Tab. 1 . The mesh definition files in *bdf*-format are available together with a definition of the connectivity between the bodies[31].

TABLE 1 Component finite element model properties

	# elements	# DOFs	$E\ [N/m^2]$	$\nu\ [/]$	$\rho\ [kg/m^3]$
Left bar	874	936	$210 \cdot 10^9$	0.288	7829
Top bar	1259	1296	$210 \cdot 10^9$	0.288	7829
Right bar	874	936	$210 \cdot 10^9$	0.288	7829

The reference multibody model is simulated using the flexible natural coordinates formulation (FNCF) which is equivalent to the classical floating-frame of reference component mode synthesis approach in the response[5]. The connection between the components is accounted for through eight spherical joints. These joints are positioned between colinear nodes of the bodies on the four revolute axes. For this particular case, no rigid or flexible spiders are employed. For the flexible body description a mode set consisting of fixed-fixed eigenmodes and constraint modes is employed. For each body four eigenmodes are used together with $4 \times 3 = 12$ constraint modes. After removal of the six rigid body modes, this leads to a total of 10 flexible deformation modes for each body. For the full mechanism this mounts up to a total of 18 rigid body DOFs and 30 flexible DOFs in the FFR-CMS description. Due to the specific structure of the FNCF approach, it has a total of 336 DOFs. These DOFs result on the one hand from the use of a full rotation matrix for the orientation parameterization, and on the other hand from the extension of each flexible mode into nine equivalent modes to account for the rotation. For the application of the joint constraints $8 \times 3 = 18$ Lagrange multipliers are employed. As has been shown before, see Vermaut *et al.*[5], this FNCF approach provides the same result as a regular FFR approach.

The simulation starts from a static equilibrium configuration, such that the initial configuration can serve for $\boldsymbol{\rho}$. To drive the mechanism, an external force with a constant amplitude of $5N$ is applied at the top right connection point of the first bar. For

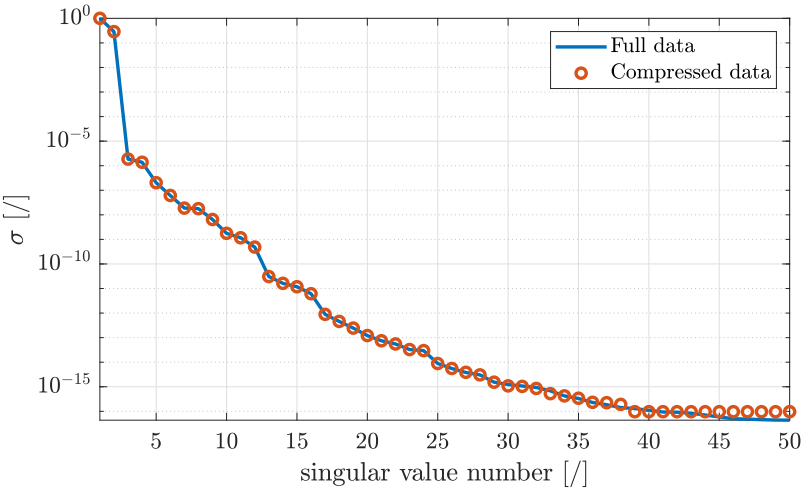

FIGURE 3 Singular values for full and compressed multibody simulation response.

the time integration of the reference model, a variable timestep BDF integrator for index-3 differential-algebraic equations is employed[32].

The SLAP models are implemented in the same multibody toolbox but employ an explicit central difference time-integrator with a constant time step of $\Delta t = 10^{-6} s$ to demonstrate the exploitation of the ordinary differential structure of the SLAP models.

6.2 | Reconstructive results

For the validation of the proposed approach, we first consider the singular value decomposition of the reference simulation. Fig. 3 shows the singular values of the full system response $\mathbf{X}^{tr,\Delta}$ as well as the compressed data set $\hat{\mathbf{Q}}^{tr}$. This figure demonstrates that, as expected, the singular values are indeed preserved under this compression operation. This compression obviously leads to a considerable reduction in the computational load for the evaluation, more precisely 0.05seconds versus 0.01seconds for this small scale example. These gains will further increase for more models with more bodies and more finely meshed components. For this mechanism for which the rigid motion will be planar as a result of the applied constraints, two modes should be sufficient to describe the main rigid portion of the motion. This is also visible in this singular value decomposition, where the first two modes have a considerably larger contribution than the other modes.

Finally the accuracy and convergence characteristics of the proposed SLAP approach are considered. First we consider the overall error on the SLAP response ϵ as a function of the number of SLAP modes m in Fig. 4 . The error ϵ is defined as the summed squared difference between the full order FNCF motion and SLAP motion for all nodal DOFs:

$$\epsilon = \sum_{j=1}^{n^t} \sum_{i=1}^{n} \left(\mathbf{x}_i(t_j) - \boldsymbol{\rho}_i - \boldsymbol{\Phi}_i^{\mathrm{sl}} \mathbf{q}(t_j) \right)^2, \tag{70}$$

with n^t the number of extracted time steps from the simulation, which is sampled at $\Delta t = 10^{-3} s$ for all simulations. This figure shows that initially a fast convergence is obtained after which the response deteriorates when the number of SLAP modes is increased. As is discussed later, this increasing error is related to the inability of the the ROB to eliminate the constrained motions from the model when the SLAP order gets too large. For the accurate, lower order SLAP simulations the detailed motion of the force application point is shown in Fig. 5 . These figures show the that in all these cases, the overall motion of the FNCF model is well approximated. However, the x-axis motion, which is purely caused due to flexible effects clearly requires a higher number of modes for an accurate representation. It is visible that these flexible effects are more accurately approximated as the number of modes increases. For reference, Fig. 6 also compares three full system configurations during the simulation for the SLAP model with $m = 6$. This figure also demonstrates the good accuracy of the SLAP model as all the nodes are visually coincident throughout the simulation.

It is interesting, contrary to common model order reduction schemes, to notice that the number of selected modes should remain limited. This is to prevent the addition of rigid body modes which should be eliminated through the reduction process,

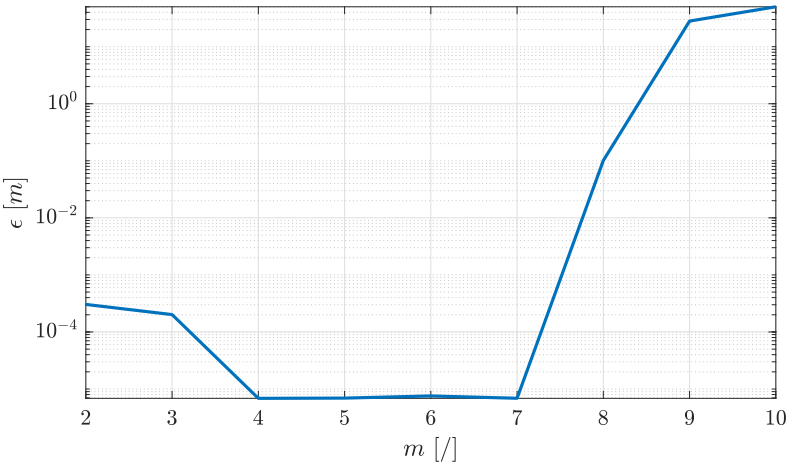

FIGURE 4 SLAP model approximation error as a function of the selected number of SLAP modes.

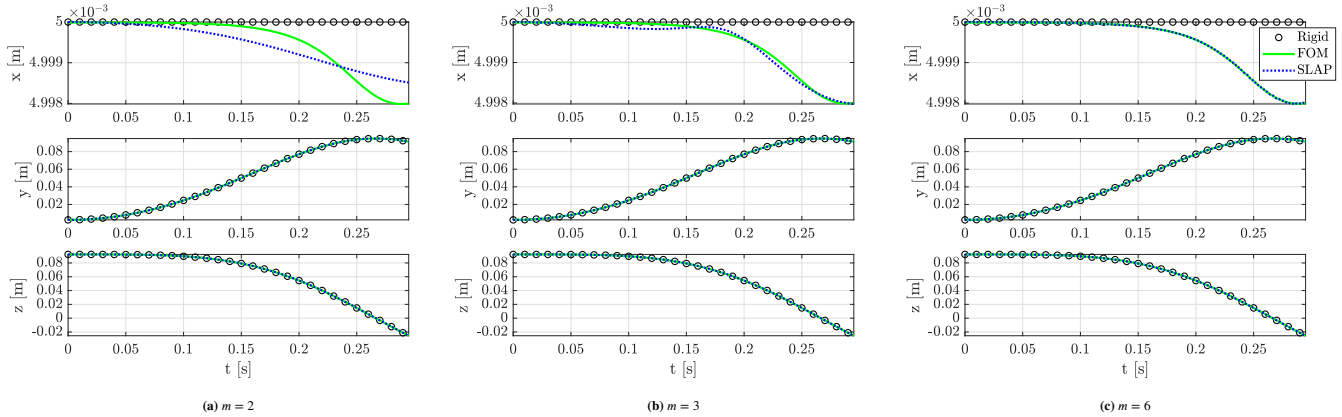

FIGURE 5 Load application point response comparison for a rigid model, the reference FNCF model and the proposed SLAP model for different orders.

as discussed in Sec. 3.3. This also explains why the error starts increasing again when the number of SLAP modes increases beyond $m = 7$ in Fig. 4 . To demonstrate the appearance of undesired rigid body modes in this case, we show the obtained system configurations for $m = 10$ SLAP modes in Fig. 7 . Here it is apparent that the joint constraints are no longer satisfied. In order to analyse the root of this issue, and the counter-intuitive divergence for larger ROM sizes, we consider the constraint violation of the different motion modes. As discussed in Sec. 3.3, the system level modes $\mathbf{\Phi}^{\text{sl}}$ should comply with the constraint Jacobian $\mathbf{C}$:

$$\mathbf{C}\mathbf{\Phi}^{\text{sl}} = \mathbf{0}. \tag{71}$$

However, due to the finite tolerance with which the constraints are met in the training simulation (as highlighted in Sec. 5.1), this equality will not hold in practice and will only be approximately true. In fig. 8 we show the joint constraint error ϵ^{joint} for each computed mode $\boldsymbol{\phi}^{\text{sl}}$ from the SVD, defined as:

$$\epsilon^{joint} = \left(\mathbf{C}\boldsymbol{\phi}^{\text{sl}}\right)^T \left(\mathbf{C}\boldsymbol{\phi}^{\text{sl}}\right). \tag{72}$$

This figure clearly shows that up to the sixth motion mode, the error on the constraint remains very small, but from the seventh mode onwards a significant error for each mode is obtained. This would not necessarily be an issue if these would correspond to (very) stiff motion modes. It is therefore interesting to also assess how the eigenfrequencies of the SLAP model evolve for a varying reduced order model size m. The eigenfrequencies for the linearized SLAP model at the initial (undeformed) configuration $\boldsymbol{\rho}$ are shown in Fig. 9 . This figure shows that initially (grey curves) only a single rigid (low frequency) mode is

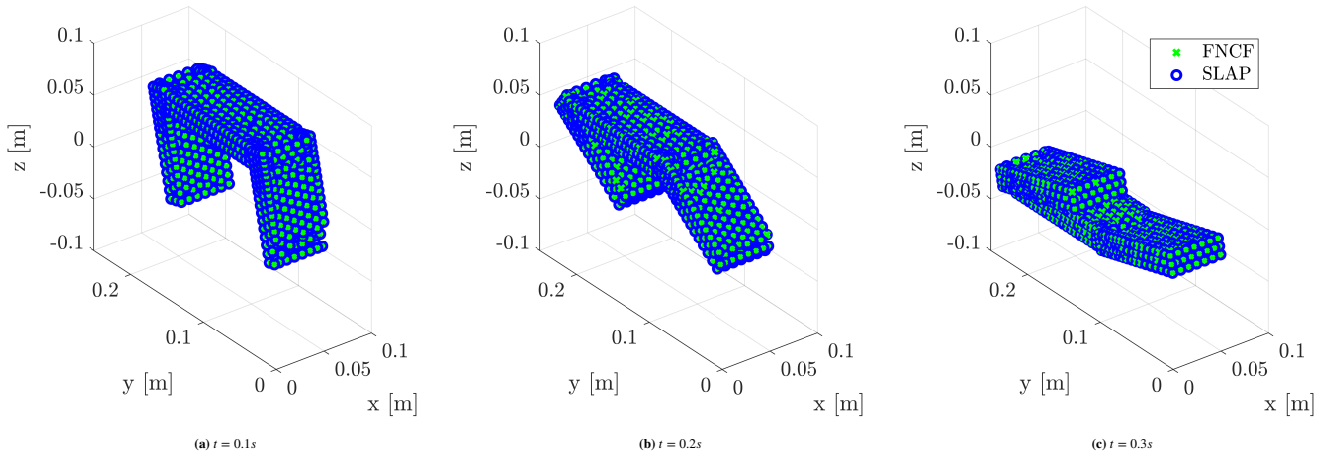

FIGURE 6 FNCF and SLAP configurations for $m = 6$ in reconstructive simulation.

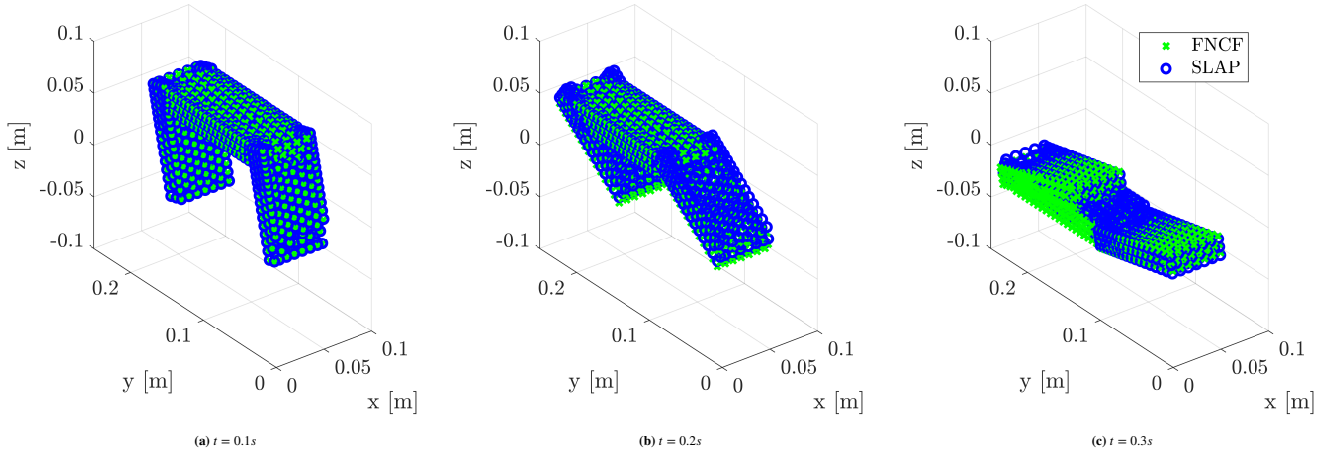

FIGURE 7 FNCF and SLAP configurations for $m = 10$, showing an undesired rigid motion contribution in the SLAP model in the reconstructive simulation.

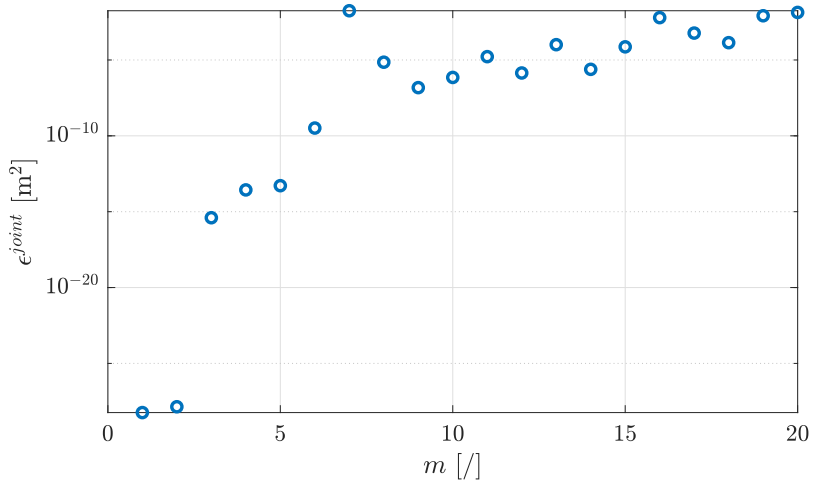

FIGURE 8 Constraint violation for computed motion modes from singular value decomposition on training simulation.

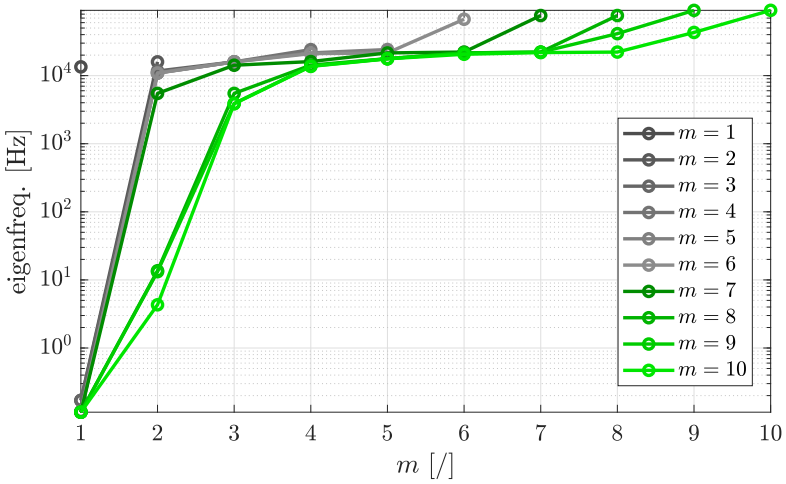

FIGURE 9 SLAP model eigenfrequencies for an increasing reduced order model size.

identified and the first eigenfrequencies converge up to $m = 6$. However, from the seventh mode onwards (green curves), the SLAP model starts to converge to a second low frequency mode. And as shown in Fig. 8 , these modes also correspond to a higher constraint violation, implying that these are spurious (close-to-)rigid body modes. However, due to their low dynamic stiffness, these modes will have a relatively large contribution to the system response and will therefore lead to large model errors. These observations indicate the importance of conducting a reconstructive simulation with the SLAP model during setup, or an analysis of the eigenfreqencies, to ensure no spurious rigid body modes appear.

6.3 | Predictive results

Finally we also consider the performance of the methodology for a predictive simulation. For the predictive case we consider the load force for the training applied in the opposite direction. This will cause the mechanism to move in the opposite direction such that overall (rigid) configurations are encountered which were not visited during the training simulation. For the SLAP model, the model with $m = 6$, which provided the best accuracy before, is considered. For this reversed load, the configuration of the mechanism at three time samples, is shown in Fig. 10 . This figure shows that the general motion of the system is accurately

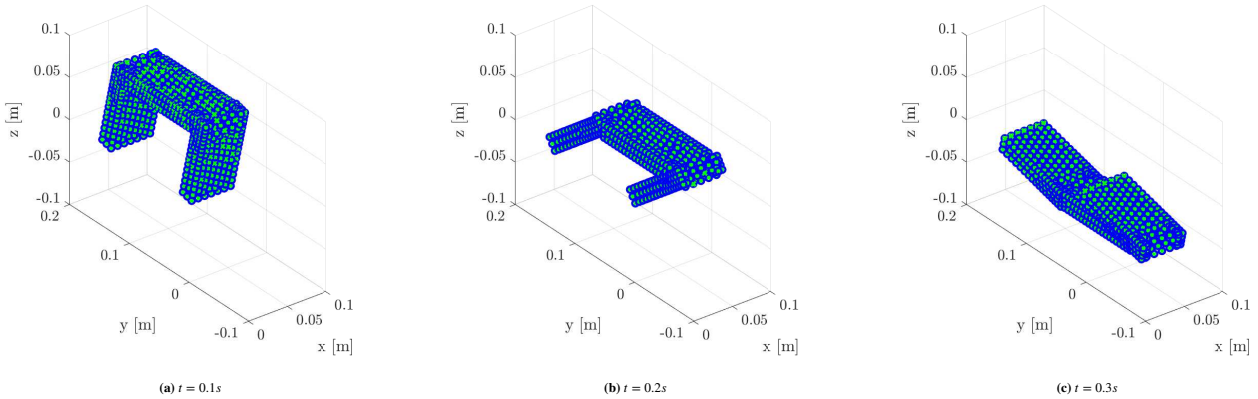

FIGURE 10 FNCF and SLAP configurations for $m = 6$ during a predictive simulation with a reversed load.

approximated with the previously defined reduced order model. For a better view of the approximation of the flexibility, we consider again the motion of the load applicaton node in Fig. 11 . From this analysis is clear that the obtained SLAP model

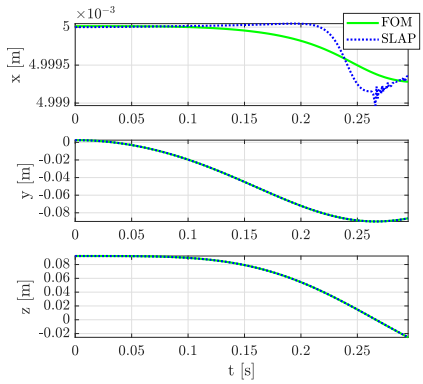

FIGURE 11 Predictive response of load application node with $m = 6$.

provides good predictive capabilities with respect to the overall motion of the system. This can be expected as for the particular case of a single degree-of-freedom mechanism performing a planar motion, the full configuration space can be described from two modes. However, the limited training set for this example does not allow to effectively describe different types of flexible deformation, and only order of magnitude trends are captured for the predictive reduced order simulation. This is what can be expected from a training based method, and demonstrates the importance of selecting an appropriate training data set which is expected to cover the relevant motion space. The practical implications will however be strongly case dependent and are not explored further in this work.

In the presented implementation, the SLAP model does not lead to lower simulation times than the reference models as the smaller timestep required by the fixed timestep central difference integrator with respect to the reference variable-timestep BDF integrator offsets potential speed gains from the new methodology. The aim is however to highlight that the SLAP formulation practically allows to evaluate the flexible multibody model in an explicit time integrator without any modifications, such that deployment in novel applications like state-estimation and optimal control becomes feasible through this new scheme.

7 | CONCLUSION

A constant reduced order basis scheme is presented for the full-system reduction of flexible multibody models. The proposed approach exploits the properties of the global nodal coordinates in order to automatically perform a data-driven constraint elimination from (a set of) training simulation(s). Due to the affine dependence between the global nodal degrees-of-freedom and the reduced order degrees-of-freedom, this approach is denoted the System Level Affine Projection (SLAP). The proposed, singular value based, reduction schemes enables an automatic joint constraint elimination for the reduced order model. As the reduction scheme is based on a singular value decomposition of the full nodal response of a flexible multibody simulation, this can pose a computational bottleneck as a dense high dimensional dataset is often obtained. An intermediate response data compression based on the component modes is proposed in order to mitigate this bottleneck, leading to low computational loads for the reduced order basis setup. The equations of motion for these new system level reduced order degrees-of-freedom are defined, and a set of ordinary differential equations with a constant, configuration independent, mass matrix and nonlinear internal forces is obtained. The resulting equations of motion computational load is independent from the original flexible multibody model size and can be obtained non-invasively with respect to the training flexible multibody software. The proposed approach is numerically validated on a flexible four bar mechanism. The SLAP approach is shown to exhibit fast convergence, also including the flexible deformation. Care must be taken however in increasing the number of reduced order DOFs, as spurious rigid body modes, resulting from a finite joint constraint accuracy, can lead to erroneous results. Future research will focus on the deployment of the SLAP approach for more generalized joint constraint conditions and more automated reduced order basis selection metrics.

ACKNOWLEDGEMENTS

The research of Frank Naets is funded by a postdoctoral fellowship of the Fund for Scientific Research, Flanders (FWO). The Research Fund KU Leuven is gratefully acknowledged for its support. This research was partially supported by Flanders Make, the strategic research centre for the manufacturing industry. The authors Humer and Gerstmayr have been supported by the Linz Center of Mechatronics (LCM) in the framework of the Austrian COMET-K2 programme.

References

1. Yoo WS, Haug EJ. Dynamics of flexible mechanical systems using vibration and static correction modes. *Journal of Mechanisms, Transmissions, and Automation in Design.* 1986;108(3):315–322.

2. Shabana A. A.. *Dynamics of multibody systems*. Cambridge: Cambridge University Press; 2005.

3. Gerstmayr J., Ambrosio J. A. C.. Component mode synthesis with constant mass and stiffness matrices applied to flexible multibody systems. *Int. J. for numerical methods in engineering.* 2008;73, pp.1518-1546.

4. Pechstein A., Reischl D., Gerstmayr J.. A Generalized Component Mode Synthesis Approach for Flexible Multibody Systems With a Constant Mass Matrix. *J. Comput. Nonlinear Dynam.*. 2013;8(1):011019.

5. Vermaut Martijn, Naets Frank, Desmet Wim. A Flexible Natural Coordinates Formulation (FNCF) for the efficient simulation of small-deformation multibody systems. *International Journal for Numerical Methods in Engineering.* 2018;115(11):1353–1370.

6. Cuadrado J., Dopico D., Barreiro A., Delgado E.. Real-time state observers based on multibody models and the extended Kalman filter. *Journal of Mechanical Science and Technology.* 2009;23(4):894–900.

7. Naets Frank, Pastorino Roland, Cuadrado Javier, Desmet Wim. Online state and input force estimation for multibody models employing extended Kalman filtering. *Multibody System Dynamics.* 2014;32(3):317–336.

8. Risaliti Enrico, Tamarozzi Tommaso, Vermaut Martijn, Cornelis Bram, Desmet Wim. Multibody model based estimation of multiple loads and strain field on a vehicle suspension system. *Mechanical Systems and Signal Processing.* 2019;123:1–25.

9. Seifried Robert. *Dynamics of underactuated multibody systems*. Springer; 2014.

10. Lehner M., Eberhard P.. A two-step approach for model reduction in flexible multibody dynamics. *Multibody Syst Dyn.* 2007;17(2-3):157–176.

11. Fehr J., Eberhard P.. Simulation Process of Flexible Multibody Systems with Non-modal Model Order Reduction Techniques. *Multibody Syst. Dyn.*. 2011;25(3):313–334.

12. Siemens Advanced Analysis User's Guide https://docs.plm.automation.siemens.com/data_services/resources/nxnastran/12/help/tdoc/e 2019-07-24; .

13. Brüls O., Duysinx P., Golinval J-C.. The global modal parameterization for nonlinear model-order reduction in flexible multibody dynamics. *Int. J. Numer. Meth. Engng.* 2007;69(5):948-977.

14. Naets F., Heirman G. H. K., Vandepitte D., Desmet W.. Inertial force term approximations for the use of Global Modal Parameterization for planar mechanisms. *Int. J. Numer. Meth. Engng.* 2010;85:518-536.

15. Naets F., Desmet W.. Super-Element Global Modal Parameterization for Efficient Inclusion of Highly Nonlinear Components In Multibody Simulation. *Multibody System Dynamics.* 2014;31(1):3–25.

16. Wu L., Tiso P., Tatsis K., Chatzi E., Keulen F.. A modal derivatives enhanced Rubin substructuring method for geometrically nonlinear multibody systems. *Multibody system dynamics.* 2019;45(1):57–85.

17. Tang Yixuan, Hu Haiyan, Tian Qiang. Model order reduction based on successively local linearizations for flexible multibody dynamics. *International Journal for Numerical Methods in Engineering.* 2019;118(3):159–180.

18. Hou Yunsen, Liu Cheng, Hu Haiyan. Component-level proper orthogonal decomposition for flexible multibody systems. *Computer Methods in Applied Mechanics and Engineering.* 2020;:112690.

19. Zwölfer A., Gerstmayr J.. Co-rotational formulations for 3D flexible multibody systems: A nodal-based approach. In: Altenbach Holm, Irschik Hans, Matveenko Valery P., eds. *Contributions to Advanced Dynamics and Continuum Mechanics*, Cham: Springer International Publishing 2019 (pp. 243–263).

20. Chatterjee A.. An introduction to the proper orthogonal decomposition. *Current Science.* 2000;78:808-817.

21. Everson Richard, Sirovich Lawrence. Karhunen–Loeve procedure for gappy data. *JOSA A.* 1995;12(8):1657–1664.

22. Halko Nathan, Martinsson Per-Gunnar, Tropp Joel A. Finding structure with randomness: Probabilistic algorithms for constructing approximate matrix decompositions. *SIAM review.* 2011;53(2):217–288.

23. Himpe Christian, Leibner Tobias, Rave Stephan. Hierarchical approximate proper orthogonal decomposition. *SIAM Journal on Scientific Computing.* 2018;40(5):A3267–A3292.

24. Besselink B., Tabak U., Lutowska A., et al. A comparison of model reduction techniques from structural dynamics, numerical mathematics and systems and control. *Journal of Sound and Vibration.* 2013;332(19):4403-4422.

25. Zwölfer Andreas, Gerstmayr Johannes. Selection of generalized component modes for modally reduced flexible multibody systems. In: ; 2018.

26. Zwölfer A., Gerstmayr J.. Preconditioning strategies for linear dependent generalized component modes in 3D flexible multibody dynamics. *Multibody System Dynamics.* 2019;47(1):65–93.

27. Brüls O., Arnold M.. The generalized-alpha scheme as a linear multistep integrator: Towards a general mechatronic simulator. *ASME Journal of Computational and Nonlinear Dynamics.* 2008;3(4).

28. Humer F., Desmet W., Gerstmayr J.. A generalized component mode synthesis approach for global modal parameterization in flexible multibody dynamics. In: ; 2014.

29. Farhat C., Avery P., Chapman T., Cortial J.. Dimensional reduction of nonlinear finite element dynamic models with finite rotations and energy-based mesh sampling and weighting for computational efficiency. *International Journal for Numerical Methods in Engineering.* 2014;98(9):625-662.

30. Vermaut Martijn, Tamarozzi Tommaso, Naets Frank, Desmet Wim. Development of a flexible multibody simulation package for in-house benchmarking. In: :1560–1571International Center for Numerical Methods in Engineering (CIMNE); 2015.

31. https://github.com/FrankNaets/SLAPPaperMeshFilesAccessed: 2019-07-24; .

32. Arévalo Carmen, Lötstedt Per. Improving the accuracy of BDF methods for index 3 differential-algebraic equations. *BIT Numerical Mathematics.* 1995;35(3):297–308.

33. Schönemann Peter H. A generalized solution of the orthogonal procrustes problem. *Psychometrika.* 1966;31(1):1–10.

How to cite this article: F. Naets, T. Devos, A. Humer, and J. Gerstmayr(2018), A non-invasive system-level model order reduction scheme for flexible multibody simulation, *Int. J. Num. Meth. Engng.*, .

APPENDIX

A SINGULAR VALUE PRESERVATION UNDER ORTHONORMAL TRANSFORMATION

In this appendix we show how an orthonormal transformation which spans the full data space preserves the singular values of that data space. Consider the singular value decomposition of a matrix $\mathbf{A} \in \mathbb{R}^{n \times n^t}$:

$$\mathbf{A} = \text{svd}(\mathbf{A}) = \mathbf{W}\Sigma\mathbf{V}^T, \tag{A1}$$

with

- $\mathbf{W} \in \mathbb{R}^{n \times n}$ and $\mathbf{W}^T\mathbf{W} = \mathbf{I}$;
- $\Sigma \in \mathbb{R}^{n \times n}$ a diagonal matrix with n singular values σ_i on its diagonal;
- $\mathbf{V} \in \mathbb{R}^{n^t \times n}$ with $\mathbf{V}^T\mathbf{V} = \mathbf{I}$,

where we assume $n^t \geq n$, but all derivations can be trivially repeated for $n^t \leq n$. We define an orthonormal matrix $\mathbf{\Psi} \in \mathbb{R}^{n \times n^m}$, for which $\mathbf{A}_i \in \text{span}\,(\mathbf{\Psi})$ for all columns i of $\mathbf{A}$ and where $n^m \leq n^t$. From this orthonormal matrix we also define the projected matrix:

$$\hat{\mathbf{A}} = \mathbf{\Psi}^T\mathbf{A}, \tag{A2}$$

with the associated SVD:

$$\hat{\mathbf{A}} = \text{svd}(\hat{\mathbf{A}}) = \hat{\mathbf{W}}\hat{\Sigma}\hat{\mathbf{V}}^T. \tag{A3}$$

We will now show that:

$$\sigma_i = \hat{\sigma}_i \quad \forall i \leq n^m, \tag{A4}$$

$$\sigma_i = 0 \quad \forall i > n^m, \tag{A5}$$

and hence the singular value decomposition of the projected matrix can be used interchangeably to perform an approximate order reduction.

From the definition of $\mathbf{\Psi}$, it follows that:

$$\mathbf{A} \in \text{span}\,(\mathbf{\Psi}) \quad \Leftrightarrow \quad \mathbf{A} = \mathbf{\Psi}\hat{\mathbf{A}}. \tag{A6}$$

By definition, this implies that the condition from Eq. (A5) is met as otherwise not all of $\mathbf{A}$ would be in the span of $\mathbf{\Psi}$. Equivalently from Eqs. (A1), (A3) we can now transform the equality from Eq. (A6) to the respective SVDs:

$$\mathbf{W}\Sigma\mathbf{V}^T = \begin{bmatrix}\mathbf{W}_{1-n^m} & \mathbf{W}_{(n^m+1)-n}\end{bmatrix} \begin{bmatrix}\Sigma_{1-n^m} & \mathbf{0} \\ \mathbf{0} & \mathbf{0}\end{bmatrix} \begin{bmatrix}\mathbf{V}_{1-n^m} & \mathbf{V}_{(n^m+1)-n}\end{bmatrix}^T = \mathbf{\Psi}\hat{\mathbf{W}}\hat{\Sigma}\hat{\mathbf{V}}^T, \tag{A7}$$

where the contributions from the zero singular values can be omitted such that:

$$\mathbf{W}_{1-n^2}\Sigma_{1-n^2}\mathbf{V}^T_{1-n^2} = \mathbf{\Psi}\hat{\mathbf{W}}\hat{\Sigma}\hat{\mathbf{V}}^T. \tag{A8}$$

From the definition of the SVD of $\hat{\mathbf{A}}$ we know that $\hat{\Sigma}$ is a diagonal matrix with the singular values $\hat{\sigma}$ on its diagonal and $\hat{\mathbf{V}}^T\hat{\mathbf{V}} = \mathbf{I}$. From the definition of $\mathbf{\Psi}$, as being orthonormal, and $\hat{\mathbf{W}}$ it also follows that:

$$\left(\mathbf{\Psi}\hat{\mathbf{W}}\right)^T \mathbf{\Psi}\hat{\mathbf{W}} = \mathbf{I}. \tag{A9}$$

hence we can substitute $\mathbf{\Psi}\hat{\mathbf{W}} = \mathbf{W}_{1-n^m}$ such that, when omitting the zero contributions, a SVD of $\mathbf{A}$ is reconstructed from the SVD of $\hat{\mathbf{A}}$. Therefore it holds that the singular values $\hat{\Sigma} = \Sigma_{1-n^m}$, such that condition Eq. (A4) is also shown. The singular value decomposition of a matrix $\mathbf{A}$ obtained from an orthonormal projection of that matrix on a basis $\mathbf{\Psi}$ with the same span can therefore be used interchangeably to determine the dominant contributions to that matrix $\mathbf{A}$.

B OPTIMAL BODY ROTATION MATRIX

In this work we exploit a novel approach for expressing the body attached reference frame in an optimal averaged sense, in contrast to previous work on absolute coordinate formulation where a rotation based on on three points was used[3,4]. This body-averaged approach has the important benefit that it is a better approximation for the Buckens frame approach typically adopted

in FFR-CMS than a three-point approach. Moreover, the approach outlined here allows to obtain the optimal averaged rotation at a computational cost independent of the original model size. The proposed methodology practically serves as an alternative to the SVD based approach for solving the *Procrustes* problem[33] and it allows to readily obtain the rotation derivatives required for evaluating the internal forces.

As discussed in Sec. 4.3 the reference body translation $\mathbf{x}_i^t \in \mathbb{R}^3$ for body i is obtained as the average displacement of the body nodes:

$$\mathbf{x}_i^t = \frac{1}{2}\sum_{j=1}^{n_i^n} \mathbf{x}_{ij} - \mathbf{x}_{ij}^0 = \mathbf{\Phi}_i^{\mathrm{sl,t}}\boldsymbol{\eta}, \tag{B10}$$

for an initially centered mesh.

In order to determine the body i rotation matrix $\mathbf{R}_i \in \mathbb{R}^{3\times3}$ we aim to find the rotation which minimizes the body deformation as defined in Eq. (51):

$$\min_{\mathbf{R}_i\in\mathbb{R}^{3\times3}} \sum_{j=1}^{n_i^n} |\mathbf{R}_i(\boldsymbol{\rho}_{ij}^c + \mathbf{\Phi}_{ij}^{\mathrm{sl,c}}\boldsymbol{\eta}) - \mathbf{x}_{ij}^0|_2 \qquad \text{s.t. } \mathbf{R}_i^T\mathbf{R}_i = \mathbf{I}. \tag{B11}$$

This goal function from Eq. (B11) can be expanded into:

$$\sum_{j=1}^{n_i^n} |\mathbf{R}_i(\boldsymbol{\rho}_{ij}^c + \mathbf{\Phi}_{ij}^{\mathrm{sl,c}}\boldsymbol{\eta}) - \mathbf{x}_{ij}^0|_2 = \sum_{j=1}^{n_i^n} \left(\mathbf{R}_i(\boldsymbol{\rho}_{ij}^c + \mathbf{\Phi}_{ij}^{\mathrm{sl,c}}\boldsymbol{\eta}) - \mathbf{x}_{ij}^0\right)^T \left(\mathbf{R}_i(\boldsymbol{\rho}_{ij}^c + \mathbf{\Phi}_{ij}^{\mathrm{sl,c}}\boldsymbol{\eta}) - \mathbf{x}_{ij}^0\right) \tag{B12}$$

$$= \sum_{j=1}^{n_i^n} (\boldsymbol{\rho}_{ij}^c + \mathbf{\Phi}_{ij}^{\mathrm{sl,c}}\boldsymbol{\eta})^T\mathbf{R}_i^T\mathbf{R}_i(\boldsymbol{\rho}_{ij}^c + \mathbf{\Phi}_{ij}^{\mathrm{sl,c}}\boldsymbol{\eta}) - 2\left(\mathbf{x}_{ij}^0\right)^T\mathbf{R}_i(\boldsymbol{\rho}_{ij}^c + \mathbf{\Phi}_{ij}^{\mathrm{sl,c}}\boldsymbol{\eta}) + \left(\mathbf{x}_{ij}^0\right)^T\mathbf{x}_{ij}^0 \tag{B13}$$

$$= \sum_{j=1}^{n_i^n} -2\left(\mathbf{x}_{ij}^0\right)^T\mathbf{R}_i(\boldsymbol{\rho}_{ij}^c + \mathbf{\Phi}_{ij}^{\mathrm{sl,c}}\boldsymbol{\eta}) + (\boldsymbol{\rho}_{ij}^c + \mathbf{\Phi}_{ij}^{\mathrm{sl,c}}\boldsymbol{\eta})^T(\boldsymbol{\rho}_{ij}^c + \mathbf{\Phi}_{ij}^{\mathrm{sl,c}}\boldsymbol{\eta}) + \left(\mathbf{x}_{ij}^0\right)^T\mathbf{x}_{ij}^0. \tag{B14}$$

In order to obtain this expansion we exploited the fact that the rotation matrix $\mathbf{R}$ has to be orthonormal (which is explicitly enforced through the constraint). From the perspective of finding the optimal rotation $\mathbf{R}_i$, the terms independent of the rotation matrix in this goal function can be omitted without influencing the minimizer. The optimization problem Eq. (B11) can therefore be rewritten as:

$$\min_{\mathbf{R}_i\in\mathbb{R}^{3\times3}} \sum_{j=1}^{n_i^n} -2\left(\mathbf{x}_{ij}^0\right)^T\mathbf{R}_i(\boldsymbol{\rho}_{ij}^c + \mathbf{\Phi}_{ij}^{\mathrm{sl,c}}\boldsymbol{\eta}) \qquad \text{s.t. } \mathbf{R}^T\mathbf{R} = \mathbf{I}. \tag{B15}$$

However, the fact that this problem is linear in the rotation matrix and redundantly constrained makes it relatively challenging to solve. However, in the following paragraph we show that this can be converted into a trivial problem by using Euler parameters to describe the rotation, rather than optimizing the full rotation matrix.

The Euler parameters $\mathbf{p} \in \mathbb{R}^4$ for body are a redundant rotational description with constraint $\mathbf{p}^T\mathbf{p} = 1$. For convenience we write:

$$\mathbf{p} = \begin{bmatrix} a \\ b \\ c \\ d \end{bmatrix}, \tag{B16}$$

and the rotation matrix as a function of these Euler parameters is obtained as:

$$\mathbf{R}(\mathbf{p}) = \begin{bmatrix} a^2+b^2-c^2-d^2 & 2bc-2ad & 2bd+2ac \\ 2bc+2ad & a^2-b^2+c^2-d^2 & 2cd-2ab \\ 2bd-2ac & 2cd+2ab & a^2-b^2-c^2+d^2 \end{bmatrix}, \tag{B17}$$

which can also be written as:

$$\mathbf{R}(\mathbf{p}) = \sum_{k=1}^{4}\sum_{l=1}^{4} \frac{\partial^2\mathbf{R}}{\partial\mathbf{p}_k\partial\mathbf{p}_l}\mathbf{p}_k\mathbf{p}_l = \sum_{k=1}^{4}\sum_{l=1}^{4} \mathbf{S}_{kl}\mathbf{p}_k\mathbf{p}_l, \tag{B18}$$

with $\mathbf{S}_{kl}$ a set of sixteen constant three-by-three matrices. The optimization problem from Eq. (B15) can now be rewritten for the Euler parameters $\mathbf{p}$ for body i:

$$\min_{\mathbf{p}\in\mathbb{R}^4} \sum_{j=1}^{n_i^n} -\left(\mathbf{x}_{ij}^0\right)^T \mathbf{R}(\mathbf{p}_i)(\boldsymbol{\rho}_{ij}^c + \boldsymbol{\Phi}_{ij}^{\mathrm{sl,c}}\boldsymbol{\eta}) \qquad \text{s.t. } \mathbf{p}^T\mathbf{p} = 1. \tag{B19}$$

With the rotation matrix as defined in Eq. (B17) this becomes a quadratic minimization problem with a single constraint. Taking this into account, the problem can again be rewritten as:

$$\min_{\mathbf{p}\in\mathbb{R}^4} -\mathbf{p}^T\left(\mathbf{A}_{i\rho} + \sum_{r=1}^{m}\mathbf{A}_{ir}\boldsymbol{\eta}_r\right)\mathbf{p} \qquad \text{s.t. } \mathbf{p}^T\mathbf{p} = 1., \tag{B20}$$

with $\mathbf{A}_{i\rho} \in \mathbb{R}^{4\times4}$ and $\mathbf{A}_{ir} \in \mathbb{R}^{4\times4}$ defined as:

$$\mathbf{A}_{i\rho,kl} = \sum_{j=1}^{n_i^n} -2\left(\mathbf{x}_{ij}^0\right)^T \mathbf{S}_{kl}\boldsymbol{\rho}_{ij}^c \quad k,l = 1,2,3,4, \tag{B21}$$

$$\mathbf{A}_{ir,kl} = \sum_{j=1}^{n_i^n} -2\left(\mathbf{x}_{ij}^0\right)^T \mathbf{S}_{kl}(\boldsymbol{\Phi}_{ij,r}^{\mathrm{sl,c}}) \quad k,l = 1,2,3,4 \quad r = 1,\ldots,m. \tag{B22}$$

For the reduced reference configuration and m reduced degrees-of-freedom, these matrices can be set up during the pre-processing such that the online evaluation of the rotation matrix becomes independent of the original model size.

Through the use of a Lagrange multiplier λ, the constrained optimization problem from Eq. (B20) is cast into an unconstrained minimization problem:

$$\min_{\mathbf{p}\in\mathbb{R}^4,\lambda\in\mathbb{R}^1} -\mathbf{p}^T\left(\mathbf{A}_{i\rho} + \sum_{r=1}^{m}\mathbf{A}_{ir}\boldsymbol{\eta}_r\right)\mathbf{p} - (\mathbf{p}^T\mathbf{p} - 1)\lambda. \tag{B23}$$

The stationary points (and hence minimizers) of this problem are found from the KKT conditions:

$$\left(\mathbf{A}_{i\rho} + \sum_{r=1}^{m}\mathbf{A}_{ir}\boldsymbol{\eta}_r\right)\mathbf{p} + \lambda\mathbf{p} = 0 \tag{B24}$$

$$\mathbf{p}^T\mathbf{p} = 1. \tag{B25}$$

It is now interesting to see that this is simply the definition of a four-by-four eigenvalue problem in $\mathbf{p}$ for an eigenvalue λ. The optimal Euler angles are hence obtained by solving this small eigenvalue problem and selecting the solution corresponding to the largest positive eigenvalue. The corresponding rotation matrix for body i can then be obtained by evaluating Eq. (B17) for this solution.

Moreover, as the eigenvalue problem is linearly dependent on the reduced degrees-of-freedom $\boldsymbol{\eta}$, the derivatives of the solution of this eigenvalue problem with respect to $\boldsymbol{\eta}$ are straightforward to evaluate from:

$$\begin{bmatrix} \left(\mathbf{A}_{i\rho} + \sum_{r=1}^{m}\mathbf{A}_{ir}\boldsymbol{\eta}_r\right) - \mathbf{I}\lambda & -\mathbf{p} \\ \mathbf{p}^T & 0 \end{bmatrix} \begin{bmatrix} \frac{\partial\mathbf{p}}{\partial\boldsymbol{\eta}_r} \\ \frac{\partial\lambda}{\partial\boldsymbol{\eta}_r} \end{bmatrix} = \begin{bmatrix} \left(-\mathbf{A}_{ir} + \lambda\mathbf{I}\right)\mathbf{p} \\ 0 \end{bmatrix}, \tag{B26}$$

which again only requires the solution of a small scale five-by-five linear system for each derivative with respect to a reduced degree-of-freedom. These derivatives are required to evaluate the derivatives of the rotation matrices with respect to the reduced degrees-of-freedom, as required for evaluation of the internal forces.